

5-1-2019

OBSERVING EXOPLANET TRANSITS WITH THE CITIZEN CONTINENTAL-AMERICA TELESCOPIC ECLIPSE (CATE) EXPERIMENT TELESCOPE NETWORK

Robert A. Baer

Southern Illinois University Carbondale, rbaer@siu.edu

Follow this and additional works at: <https://opensiuc.lib.siu.edu/theses>

Recommended Citation

Baer, Robert A., "OBSERVING EXOPLANET TRANSITS WITH THE CITIZEN CONTINENTAL-AMERICA TELESCOPIC ECLIPSE (CATE) EXPERIMENT TELESCOPE NETWORK" (2019). *Theses*. 2487.
<https://opensiuc.lib.siu.edu/theses/2487>

This Open Access Thesis is brought to you for free and open access by the Theses and Dissertations at OpenSIUC. It has been accepted for inclusion in Theses by an authorized administrator of OpenSIUC. For more information, please contact opensiuc@lib.siu.edu.

OBSERVING EXOPLANET TRANSITS WITH
THE CITIZEN CONTINENTAL-AMERICA TELESCOPIC ECLIPSE (CATE)
EXPERIMENT TELESCOPE NETWORK

by

Robert Baer

B.S., Illinois State University, 1995

A Thesis

Submitted in Partial Fulfillment of the Requirements for the
Master of Science Degree

Department of Physics
in the Graduate School
Southern Illinois University Carbondale
May 2019

THESIS APPROVAL

OBSERVING EXOPLANET TRANSITS WITH THE CITIZEN
CONTINENTAL-AMERICA TELESCOPIC ECLIPSE (CATE) EXPERIMENT
TELESCOPE NETWORK

By

Robert Baer

A Thesis Submitted in Partial
Fulfillment of the Requirements
for the Degree of
Master of Science
in the field of Physics

Approved by:

Dr. Mark Byrd, Chair

Dr. Saikat Talapatra

Dr. Harvey Henson

Graduate School
Southern Illinois University Carbondale
March 1, 2019

AN ABSTRACT OF THE THESIS OF

Robert Baer, for the Master of Science degree in Physics, presented on March 1, 2019, at Southern Illinois University Carbondale.

TITLE: OBSERVING EXOPLANET TRANSITS WITH
THE CITIZEN CONTINENTAL-AMERICA TELESCOPIC ECLIPSE (CATE)
EXPERIMENT TELESCOPE NETWORK

MAJOR PROFESSOR: Dr. Mark Byrd

The Citizen Continental-America Telescopic Eclipse (CATE) Experiment established a standardized set of observation procedures and 72 volunteer observation teams with identical equipment along the path of the 2017 total solar eclipse. CATE successfully imaged the solar corona from 66 of the 72 observation sites resulting in a high dynamic range animation of 90 minutes of solar corona data collected by volunteer citizen science teams. A subgroup of CATE began work in the fall of 2017 to evaluate use of the standard CATE observation setup for exoplanet transit observations. Light curves and analysis of data using AstroImageJ of two well know transiting exoplanets, HD209458b ($V = 7.65$, depth = 1.5%) and HD189733b ($V = 7.67$, depth=2.4%) are presented along with modifications to CATE telescopes required for successful exoplanet follow up observations.

ACKNOWLEDGMENTS

I would like to thank Dr. Mark Byrd for his guidance and patience as well as the members of my graduate committee, Dr. Harvey Henson and Dr. Saikat Talapatra.

This study would have not been possible without the efforts of Citizen CATE Experiment [26] volunteers and colleagues. Special thanks to Mike Conley, Kevin Cobble, and David Elmore, who performed exoplanet observations with the CATE telescope system, and Dr. Matt Penn for his advice and guidance with this study.

Additional thanks to Dr. Dennis Conti for his work on "A Practical Guide to Exoplanet Observing," that was an invaluable resource to me in observations and data analysis.

This research has made use of AstroimageJ [9].

This research has made use of EXOFAST [11] quadratic limb darkening parameter code.

This study made use of the Exoplanet Transite Database [30] operated by the Variable Star and Planet Section of the Czech Astronomical Society.

This research has made use of the NASA Exoplanet Archive [22], which is operated by the California Institute of Technology, under contract with the National Aeronautics and Space Administration under the Exoplanet Exploration Program.

This research has made use of the SIMBAD database [35], operated at CDS, Strasbourg, France.

This research has made use of "Aladin sky atlas" [2] [1] developed at CDS, Strasbourg Observatory, France.

This research has made use of Astrometry.net [19] plate solving resources.

This research has made use of the Exoplanet Orbit Database and the Exoplanet Data Explorer at exoplanets.org [14].

This research has made use of Firecapture image capture software [12].

PREFACE

The discovery of new planets outside of our own solar system has increased significantly over the last ten years. New exoplanet surveys such as the Transiting Exoplanet Survey Satellite (TESS) [23] could discover thousands of exoplanets over the missions's lifetime. We are headed into an era where astronomers will have to prioritize planetary discoveries for follow up observations due to the large number of new discoveries and observational time constraints on professional telescopes. There is an opportunity for citizen science to make significant contributions to this field of study.

The Citizen CATE Experiment [26] established a national network of volunteer amateur astronomy teams all with identical equipment to collect data on the solar corona during the 2017 total solar eclipse. While originally designed for coronal imaging, the CATE system is capable of imaging other celestial objects.

The purpose of this study was to determine if the Citizen CATE telescope system, operated by volunteers, could successfully observe an exoplanet transit. Data was collected by four volunteer teams including the author. This study reports on observation and data collection procedures by the teams, required telescope modifications, and finally the data reduction and analysis performed by the author. The study has shown that it is possible to confirm exoplanet transits of bright stars with the CATE telescope system and is a first step towards utilizing the CATE network in support of current exoplanet observation campaigns.

TABLE OF CONTENTS

Abstract	i
Acknowledgments	ii
Preface	iii
List of Tables	vi
List of Figures	vii
1 Introduction	1
1.1 Exoplanets	1
1.1.1 Exoplanet Discovery Methods	2
1.1.2 Modeling Exoplanet Light Curves	3
1.1.3 Opportunities for Amateur Astronomers	6
1.2 The CATE Network	7
1.2.1 The CATE Instrument	8
1.2.2 Coronal Imaging Outcomes	10
2 Observing Exoplanet Transits with the CATE Instrument	11
2.1 Adapting the Scope for Night Imaging	12
2.2 Observation Limitations	14
2.3 Exoplanet Observation Candidates	14
2.3.1 Calibration Images	17
2.3.2 Test Images	18
2.3.3 Data Storage Considerations and Acquisition	18
2.4 Data Collection and Reduction	19
2.4.1 HD209458b Observation	19
2.4.2 HD189733b Observation	19
2.4.3 Data Reduction	20
2.4.4 Noise Reduction	25

3	Analysis	29
3.1	Transit Model Fitting	29
3.1.1	HD209458b	30
3.1.2	HD189733b	40
4	Summary	49
	References	51
	Vita	56

LIST OF TABLES

2.1	Observable exoplanet transits.	15
2.2	HD209458b observable transits.	16
3.1	HD209458b and HD189733b transit, orbital, and host star parameters.	30
3.2	HD209458b measured transit parameters compared to known values	39
3.3	HD189733b measured transit parameters compared to known values	48

LIST OF FIGURES

1.1	Exoplanet detections 1989 to 2018	2
1.2	Transit light curve	3
1.3	Planetary transit stages	4
1.4	Transit geometry	4
1.5	Kepler and TESS exoplanet discoveries	7
1.6	Citizen CATE Experiment observation sites for the 2017 eclipse	8
1.7	Citizen CATE Experiment coronal HDR image	10
2.1	HD189733	12
2.2	HD20948b discarded frame	20
2.3	HD209458b frames showing satellite in FOV	21
2.4	AstroImageJ aperture placement	22
2.5	AstroImageJ seeing profile of HD209458b.	23
2.6	HD209458 source and comparison stars	24
2.7	Image shifting and hot pixels.	27
2.8	HD209458b original data vs outliers removed	28
3.1	HD209458b model fitting in AstroImageJ.	31
3.2	HD209458b transit light curve, 6 comparison stars	32
3.3	HD209458b light curve	33
3.4	HD209458b light curve, 4 comparison stars	34
3.5	HD209458b model fit parameters, 4 comparison stars	35
3.6	HD209458b light curve, outliers removed	36
3.7	HD209458b model fit, 4 comparison stars	37
3.8	HD209458b light curve, 4 comparison stars, outlier data removed	38
3.9	HD189733b seeing profile	41
3.10	HD189733b target and comparison stars	42
3.11	HD189733b light curve, 8 comparison stars	43

3.12	HD189733b model fit parameters, 8 comparison stars	44
3.13	HD189733 light curve, outliers removed	45
3.14	HD189733b light curve, outliers removed	46
3.15	HD189733b model fit parameters, outliers removed.	47

CHAPTER 1

INTRODUCTION

The Citizen Continental-America Telescopic Eclipse (CATE) Experiment [26] is a volunteer based Citizen Science project to image the solar corona during the August 21, 2017 total solar eclipse. The experiment resulted in 72 trained observation teams spread throughout the U.S. roughly along the path of totality from Oregon to South Carolina. The telescope network was able to successfully image the solar corona from 66 of the 72 sites along the path of totality in 2017 resulting in a time compressed animation representing 90 minutes of coronal evolution. Of the sites not being able to collect data, one was due to mechanical failure and five were due to cloudy conditions. The next total solar eclipse observation coming up in the continental United States is not until April 8, 2024, leaving several years for the Citizen CATE network to look into other astronomy observation campaigns.

A subgroup of the CATE team consisting of Robert Baer, Kevin Cobble, Mike Conley, and David Elmore began exoplanet transit observations in December, 2017. These exoplanet observations with CATE scopes are to evaluate the feasibility of using the CATE network for follow up observations to the TESS (Transiting Exoplanet Survey Satellite) [23] mission and similar campaigns to observe exoplanet transits around relatively bright host stars. There is the potential for CATE to contribute to the discoveries by volunteer teams performing follow up observations of TESS candidates that may otherwise be unfeasible follow up targets for large telescopes operated by professional astronomy groups.

1.1 EXOPLANETS

A planet that orbits a star other than our own Sun is generally known as an exoplanet. The existence of exoplanets has been suspected for some time. However, the first detection of an exoplanet was not until 1988 by Campbell, Walker, and Yang [5].

Confirmation of the discovery came in 2002 by a team including Hatzes and Cochran [15]. Discovery of new exoplanets has increased significantly in the last decade. As of November 15, 2018, a total of 3,838 confirmed exoplanets have been discovered by numerous surveys as shown on the NASA Exoplanet Archive [22].

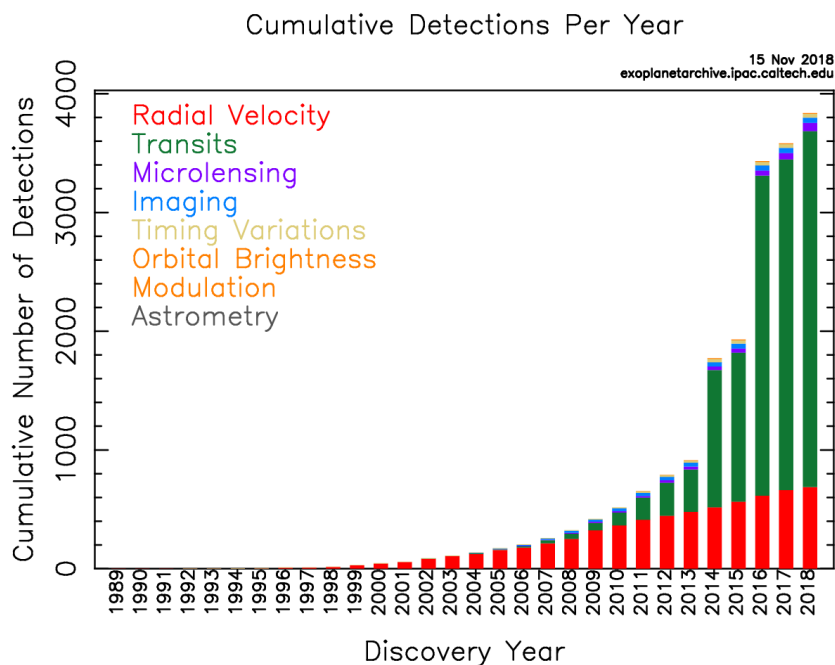


Figure 1.1. Exoplanet detections per year from 1989 to Nov 15, 2018 [22].

1.1.1 Exoplanet Discovery Methods

Exoplanet discoveries include several different methods with transit photometry being the most productive method of recent years [34] [7]. The transit method involves observing the light output of a star over time to look for a drop in the flux (light level) of the star as a planet passes between the star and observer as shown in figure 1.2. Discovery of a potential exoplanet involves plotting the flux of the star as observed over time. When a periodic dip in the flux is noticed, a potential exoplanet is flagged for follow up observations. Plots of the stars flux over the time of the transit are known as light curves. The curves contain information about the size of the planet relative to its host star as

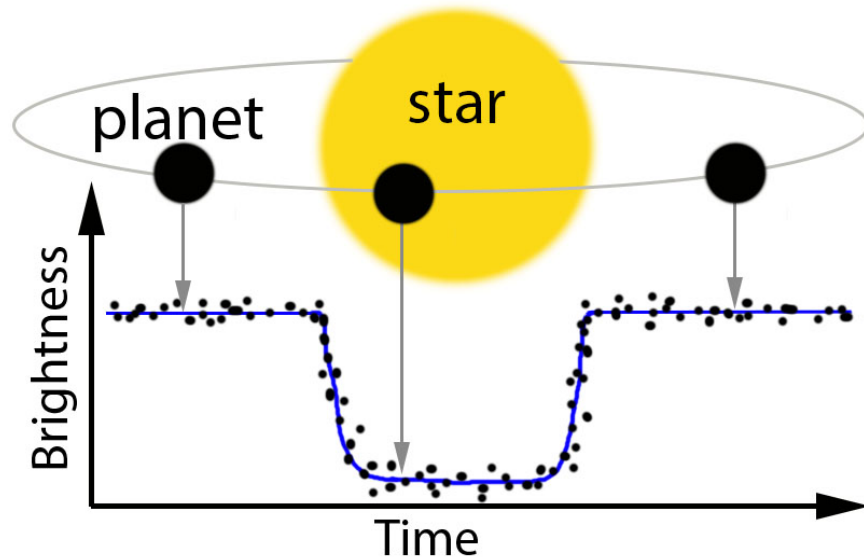


Figure 1.2. An exoplanet transit light curve showing light level before, during, and after a transit. Host star and orbiting exoplanet are represented above the light curve.

well as the length of the transit. Until very recently, exoplanet's discovered by transit method required confirmation by another detection method, typically radial velocity [7]. Morton et al., 2016 [21] was able to recently demonstrate false positive probabilities could be accurately estimated by applying code to transit data from the Kepler mission. In cases where not enough transit data has been collected to make a determination, follow up observations are needed. Analysis of photometry data by fitting the data to light curve models can be used to determine a wealth of information on the host planet and its orbit. Additionally, follow up observations of a confirmed exoplanet are necessary to further refine the transit data and keep from losing track of the transit over time.

1.1.2 Modeling Exoplanet Light Curves

Transits can be modeled as an eclipse of a star by a dark sphere. The simplest case involves a planet transiting a star of uniform brightness. Mandel and Agol [20] showed that a uniform source can be modeled as follows. The transit case discussed here will be limited to transits of planets smaller than the host star so that at no time does the planet

eclipse the entire solar disk. There are then three possible positions of the planet to consider as shown in figure 1.3.

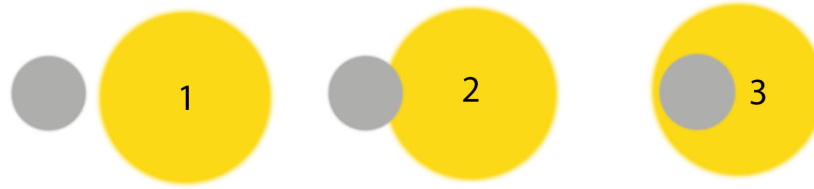


Figure 1.3. Planetary transit stages showing three possible planet locations with the planetary disk either not transiting, partially transiting, or fully inside the stellar disk.

Let the geometry of the transit be further defined. Consider a star of radius r_* and a transiting planet of radius r_p as shown in figure 1.4.

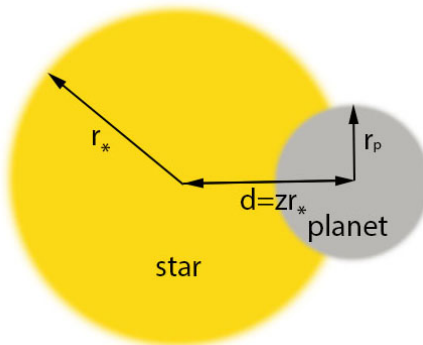


Figure 1.4. Transit geometry. A planet of radius r_p transits a star of radius r_* .

The distance between the centers of the star and the planet is $d = z r_*$ where z is the normalized separation of the centers. The ratio of planet to the star, $p = r_p / r_*$. For a uniform light source the ratio of the obscured to unobscured brightness or flux, $F_e(p, z) = 1 - \lambda_e(p, z)$ where

$$\lambda_e(p, z) = \begin{cases} 0, & 1 + p < z, \\ \frac{1}{\pi} \left[p^2 k_0 + k_1 - \sqrt{\frac{4z^2 - (1 + z^2 - p^2)^2}{4}} \right], & |1 - p| < z \leq 1 + p, \\ p^2, & z \leq 1 - p, \end{cases} \quad (1.1)$$

and $k_1 = \arccos[(1 - p^2 + z^2)/2z]$, $k_0 = \arccos[(p^2 + z^2 - 1)/2pz]$.

Figure 1.3 shows the location of the planet for each case. Case 1, $z > 1 + p$, the planet is not transiting the star. Case 2, $|1 - p| < z \leq 1 + p$, the planetary disk is partially over the stellar disk. Case 3, $z \leq 1 - p$, the planetary disk is inside the stellar disk.

The change in observed flux as the planet transits the star when plotted will result in a light curve as shown in figure 1.2. For a uniform light source, the dip in light would resemble a square wave whereas the light curve of a typical star will have a slight curve to the bottom of the dip. The curve is the result of limb darkening caused by the star being centrally brighter than at the edges. For accurate light curve modeling, limb darkening must be taken into account [20].

This study uses AstroImageJ [9], a specialized distribution of ImageJ written in Java for data reduction, transit modeling, and light curve plots. AstroImageJ is able to do very fast transit modeling by utilizing Mandel and Agol's small planet approximation taking into account limb darkening. The approximation is for $p \leq .1$, or a planet size approximately 1/10 or smaller than the host star. The approximation assumes uniform star brightness under the planet's disk for $z < 1 - p$. The flux then becomes, $F = 1 - p^2 I^*(z)/4\Omega$ where $I^*(z) = (4zp)^{-1} \int_{z-p}^{z+p} I(r) 2r dr$ and $\Omega = \sum_{n=0}^4 c_n (n+4)^{-1}$, a function of the angle between the observer and the normal to the stellar surface, taking into account optical properties of the observation system [8]. The normalized radial coordinate on the disk of the star, $0 < r < 1$, and $I(r)$ is the specific intensity as a function of r with $I(0) = 1$ [20]. When $1 - p < z < 1 + p$ the light curve can be approximated as:

$$F = 1 - \frac{I^*(z)}{4\Omega} \left[p^2 \cos^{-1} \left(\frac{z-1}{p} \right) - (z-1) \sqrt{p^2 - (z-1)^2} \right], \quad (1.2)$$

where $I^*(z) = (1-a)^{-1} \int_{z-p}^1 (I(r) 2r dr)$.

Given some information on the host star from previous studies, it is possible to attain planetary orbit information by analyzing the transit flux data. This includes the planetary orbit semi-major axis, a , inclination angle i , and z_0 , the smallest impact parameter. Additionally, the planet's radius R_p , mass M_p , average density ρ , and surface gravity can be determined from the transit data provided we have a reasonable estimate for the host star's radius R_* , stellar mass M_* , and the minimum planetary mass from radial velocity measurements [7]. The depth of the transit is defined simply as a ratio of the observed fluxes which can be described as a ratio of the planetary and stellar radii [28]:

$$\Delta F \equiv \frac{F_0 - F_{transit}}{F_{transit}} = \left(\frac{R_p}{R_*} \right)^2 \quad (1.3)$$

1.1.3 Opportunities for Amateur Astronomers

The recently launched TESS mission is expected to identify thousands of exoplanet candidates, some of which will require follow up observations [23]. Unlike previous surveys such as Kepler that looked at dim stars in a small region of the sky, the TESS mission will observe 90% of the sky and look at relatively bright stars. Compared to the Kepler mission, TESS candidate stars are on average 100X brighter, which puts them in a category of stars observable by amateur equipment such as that used by Citizen CATE.

TESS planet candidates will offer easier follow up observation targets than previous missions such as Kepler. This opens the door for follow up observations with relatively small ground-based telescopes. Equipment required to do follow up work is an imaging telescope on a relatively accurate mount with the ability to stay on target for several hours during a transit. CATE equipment with minimal modifications to the mount adding tracking and guiding ability is suitable for this type of observation. The volunteer network created by CATE offers some unique advantages over a single observer. The large

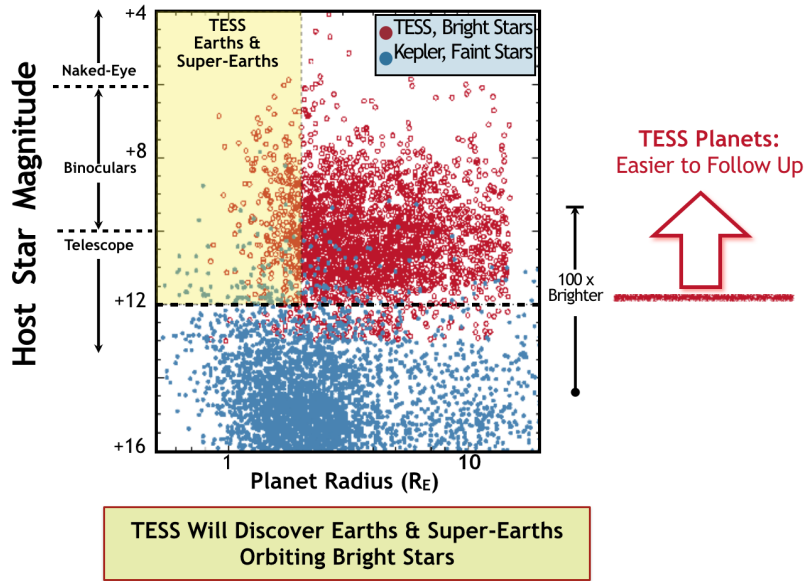


Figure 1.5. Kepler and TESS expected exoplanet discoveries. TESS host star magnitude and planet radius (red data) compared to Kepler (blue data) Image credit: MIT[23].

network can not only be used to observe a single target with a single scope, it is possible for the entire network to observe a single target with multiple (up to 72) identical ground based scopes in order to create precise light curves for follow up observations and further exoplanet classification. The observations may provide critical data to the professional astronomy community that would otherwise be impractical to gather on the larger professional telescopes due to observational time constraints.

1.2 THE CATE NETWORK

The CATE network of telescopes was originally designed to position teams roughly every 40 miles from Oregon to South Carolina in the path of the 2017 total solar eclipse. The Citizen CATE teams all kept their observation equipment after the eclipse which has resulted in the network of telescopes being intact and ready for another project. This distribution of scopes across the continental U.S. gives a large window of opportunity for observations to take place. Utilizing the entire network for observations minimizes weather issues that can block a single location. The network covers four different time

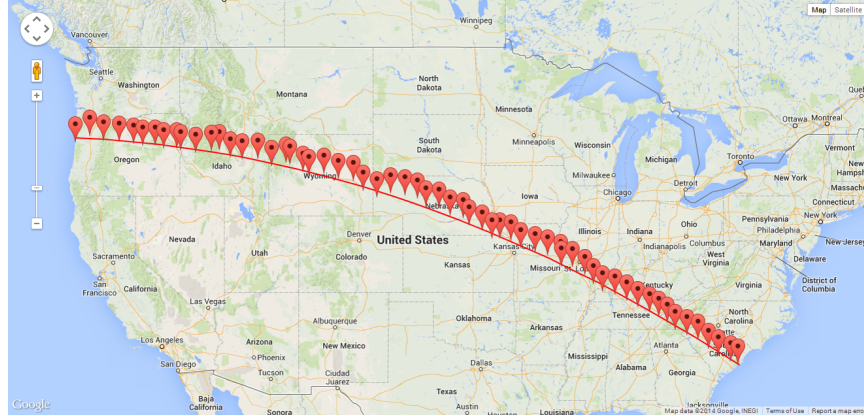


Figure 1.6. Citizen CATE Experiment observation sites for the 2017 eclipse. Image credit: Citizen CATE Team, citizencate.org

zones across the U.S. allowing for a larger number of transits to be observed in one night than from a single location.

1.2.1 The CATE Instrument

The CATE instrument is composed of off-the-shelf components consisting of a telescope, mount and drive, camera, filters, and laptop. The telescope is an 80mm, F/6.25 refractor with an extremely low dispersion doublet primary lens manufactured by Daystar Filters, LLC. It includes a 2 inch locking Crayford focuser. A two inch extension tube is attached to the focuser to provide necessary back focus for the camera, which is attached to the telescope utilizing a 1.25 inch C-mount adapter and a 2 inch to 1.25 inch converter included with the scope. Further information on the solar setup can be found in Penn et al., 2016 [26].

All CATE telescopes utilize Celestron CG4 mounts and tripods for solar observations. The right ascension (RA) drive motor and controller from the Celestron dual axis drive kit was utilized for tracking. Declination (DEC) adjustments were made manually. The drive is powered by four D-cells, which was found to operate the mount reliably for several hours. The mount utilized a pinhole style Televue Solar pointer to assist getting the scope on target. The mount has no computer controlled pointing or guiding

capabilities in the standard configuration.

The camera utilized is a Point Grey Grasshopper USB 5 Mpixel, model GS3-Us-51S5M-C. The camera uses a Sony IMX250 CMOS array. The camera is capable of up to 45 frames per second, which is limited by the speed of the computer and USB port the camera is plugged into. Camera control, exposures, and GPS time stamping for solar observations is done through an Arduino microcontroller.

A laptop was utilized for data collection with a custom MATLAB program developed by Mathworks and CATE volunteers. The software guided volunteers through all phases of data collection including taking calibration images, mount alignment, collection of science images, and data backup. The software was developed utilizing input from eclipse observation during the previous two total solar eclipses in the Faroe Islands [25] and Indonesia where volunteers imaged the eclipse utilizing Point Grey Fly Capture software and beta software being developed in MATLAB [26]. CATE teams additionally trained on using FireCapture [12] image acquisition software as a backup method in the event that primary software acquisition failed.

The entire CATE setup was designed to run from battery power in remote locations for up to 3 hours. Several volunteer groups utilized automotive 12V 30AH or larger battery packs and portable DC to AC power inverters to extend the system runtime by an additional 3 to 6 hours.

The scope setups being designed primarily for solar imaging, have no finder, and only track using the RA motor. Finding and tracking the Sun is a relatively simple procedure aided by mount alignment procedures in the MatLab Solar Eclipse Application. Polar alignment on the scopes is accomplished through pointing the mount North, and fine tuning the alignment using drift alignment techniques. For more information see Penn et al., 2015, 2016 [25] [26]. Several teams also used smart phone applications to do rough mount alignment prior to drift aligning. This alignment is sufficient for getting on the Sun and keeping the corona image centered for the few minutes needed during a total solar eclipse; however, more accurate alignment is needed for night time imaging over

several hours.

1.2.2 Coronal Imaging Outcomes

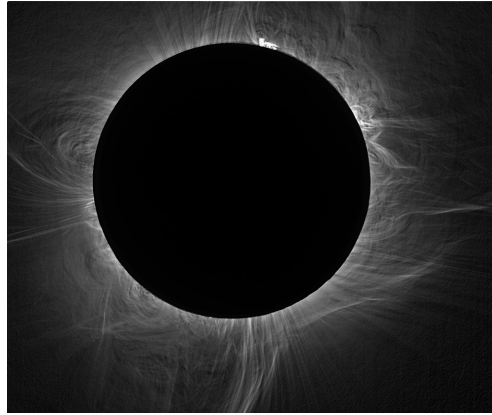


Figure 1.7. Citizen CATE Experiment coronal image March 9, 2016. HDR image stacking and Sobel edge detection filtering by D. Elmore. Additional editing by R. Baer.

CATE volunteer team success on August 21, 2017 was exceptionally high with 92% of sites collecting enough data to make at least one coronal high dynamic range (HDR) image. This high success rate further demonstrated the ability of the network to do a successful coordinated observation. Identical equipment used in all setups allow data from the sites to be combined. For the 2017 eclipse data, this means that HDR images from multiple sites can be combined together to show coronal evolution over the full 90 minutes of observations performed by the CATE network. For more information, see citizencate.org.

CHAPTER 2

OBSERVING EXOPLANET TRANSITS WITH THE CATE INSTRUMENT

The first and most obvious difference between solar observations and exoplanet transit observations is that the exoplanet transit observations take place at night. Data acquisition for both types of photometry observations consist of taking a series of images. For an exoplanet transit, the observer is imaging a part of the sky centered on the exoplanet's host star. The observation must take place during the transit, which occurs at the same time regardless of your location on earth. CATE volunteer teams became familiar with night time imaging from practicing imaging the Moon leading up to the 2017 total solar eclipse. This imaging is relatively easy to do since the Moon is a bright target requiring short exposures. Polar alignment of the mount is significantly easier at night when Polaris is visible than during the day. Drift alignment procedures developed during CATE solar observation can further be used to fine tune the polar alignment. The default sidereal tracking rate on the CG-4 mount is matched to tracking rates for stars and therefore will work well on exoplanet transits. FireCapture [12] image acquisition software, available as a free download from www.firecapture.de, is used to acquire images with all data acquisition and camera control being done through the software. Image acquisition can be automated in FireCapture allowing images to be taken at a regular interval.

Limitations of the current Citizen CATE setup become evident when trying to image dimmer and difficult to find objects. With no finder scope and no computer assisted pointing, it can be nearly impossible to find the desired exoplanet host star. If the observer can find it, tracking it successfully for the duration of the transit over several hours can be a challenge for a scope with no feedback to the tracking system. The user would need to use a bright reference star in the field of view (FOV) to manually keep the image centered. Relatively short exposures of a few seconds for star field imaging will be required in order to get enough data points to show a light curve. One can not for

example take 30 minute exposures for a 3 hour transit as the resulting light curve would only have 6 data points. Data collection for a star candidate should be done such that the exposure required to detect the star is as short as possible.

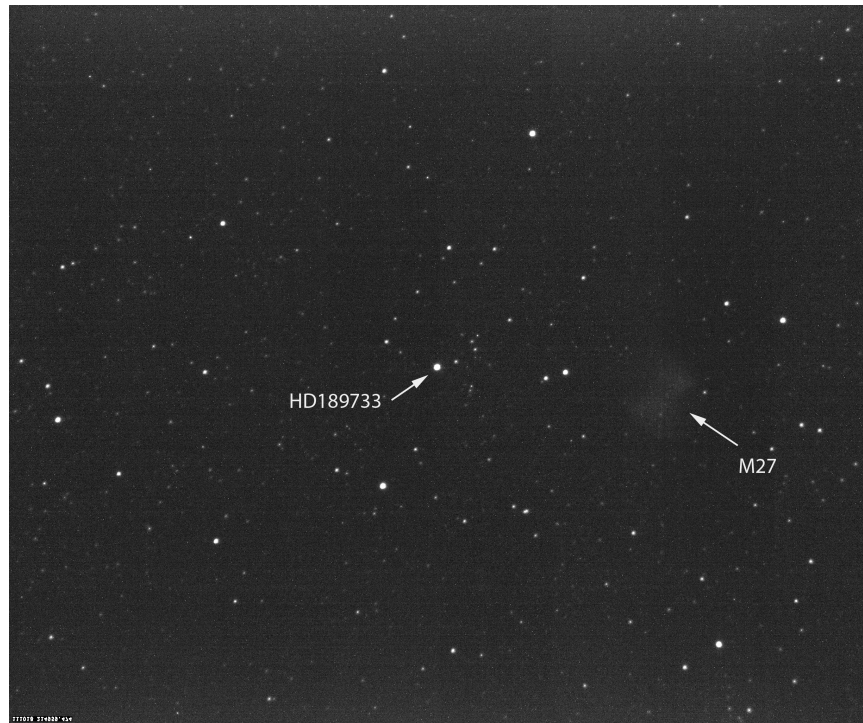


Figure 2.1. HD189733 image taken by CATE volunteer Mike Conley. HD189733 in center of image with M27, the Dumbbell Nebula shown on the right. Standard CATE imaging system, 2 second exposure.

2.1 ADAPTING THE SCOPE FOR NIGHT IMAGING

With the standard CATE mount, the observer must be able to visually find the target star. There is no computer controlled pointing capability. Finding a target can be quite difficult and time consuming especially when looking for target stars that are not visible with the unaided eye, below magnitude 6. Computer controlled pointing capability in the mount greatly simplifies the observation procedure allowing the mount to go to a target star after an initial alignment procedure. CATE volunteer Kevin Cobble created the Z-field dual axis CG4 micro controller using an Arduino micro controller. For approximately \$70 in parts, a CATE observer can assemble their own controller adding

basic pointing capability to the CG4 mount.

The dual axis controller has the ability to point accurately within about 10 degrees from a known star. It also has the ability to do feedback controlled guiding of the telescope if a second camera attached to a finder scope is used. CATE volunteer Mike Conley utilized an Orion 50mm mini guider finder scope with an Orion Starshoot Autoguider camera and PHD2 [31] guidance software. PHD2 software is free and open source. It is available from openphdguiding.org. It provides feedback to the controller as a selected guide star drifts, sending signals to the RA and DEC motors to put the telescope back on target. Due to the long data collection times, observers are required to have access to AC power or a external batteries capable of keeping all electronics running for at least six hours.

Astrometric calibration (plate solving) software from Astrometry.net [19] has been added to the CATE laptops used for exoplanet observations. Once the user thinks they are on target, they take a test image and submit it to the plate solving software. The plate solving software calculates relative positions of stars in the image and comes up with a solution, labeling brighter stars in the image. This allows the observer to verify they are on target before taking data for the evening. The software does not rely on an Internet connection. When the target is verified, guiding software is turned on and the guide star is selected. The software will then work with the controller to keep on target. With guiding turned on, the host star stays centered in the field of view (FOV) within a user specified pixel range. In the event auto guiding is not used, the user can opt to manually center the image throughout the duration of the observation. Control cables for adjustments can be rather long allowing users to sit inside a house or observing room while the telescope operates outside. This can help make observations more tolerable for volunteers during times of extreme heat or cold.

2.2 OBSERVATION LIMITATIONS

Stars down to magnitude 12 are observable in images taken with the CATE telescope using 5 second exposures and zero camera gain. Although they are observable, the star is so dim that the signal to noise ratio is very low. The brightness of the star is likely not enough for the CATE scope to detect the small changes in light when an exoplanet passes in front of the star without significant noise reduction techniques being used. Stars of magnitude 9 or greater show a high enough signal above the background to detect a transit with little to no additional noise reduction required. Clear weather is required for an extended period of time; 3-6 hours depending on the transit length. The target star must be high enough to clear the horizon, typically 20 degrees altitude or more, and observations typically need to be done at least an hour past sunset or before sunrise to allow for dark skies. The depth of the transit needs to be sufficiently large to be observable. For CATE test targets, transit depths greater than 1% were observed. A sufficient number of comparison stars similar in magnitude to the host star need to be present in the FOV. A relatively short transit of 3 hours or less was desired for this study to keep the observation sessions short. Shorter observations are much more likely to be successful than long observations which require a longer clear weather window.

2.3 EXOPLANET OBSERVATION CANDIDATES

The Exoplanet Transit Database [30] was used to review possible candidates for CATE exoplanet observations. HD209458b, 7.65 magnitude, depth 1.5%, and HD189733b 7.67 magnitude, depth 2.4% were selected. Both systems have been studied extensively and have well-known stellar and planetary parameters [3] [6] [16] [18]. Dimmer stars with known transits occurring in the same time period were also identified as secondary targets. This was done in case a primary transit was missed on a given night, the observer may be able to make use of the observation session to image a secondary transit that would be useful to the study. Primary and secondary targets for the study are shown in table 2.1.

The first exoplanet observations with the CATE equipment was done by CATE

volunteers Elmore in Colorado and Cobble in Texas of the December 2017 transit of HD209458b. Observation dates were further established for Illinois and Oregon for Baer and Conley respectively. The Exoplanet Transit Database was utilized to find predicted transit times for targets in each location.

Table 2.1. Observable exoplanet transits. Data from the Exoplanet Transit Database [30].

Observable Exoplanet Transits				
Object	V (mag)	dV (mag)	Duration (min)	Period (days)
HD209458b	7.65	0.0162	184.2	3.5247
HD189733b	7.67	0.0282	109.6	2.218
WASP-3b	10.64	0.0123	137	1.84
WASP-74b	9.7	0.0104	137.52	2.13
XO-6b	10.25	0.0131	174	3.765
WASP-14b	9.75	0.0108	167	2.24
WASP-33b	8.3	0.0151	163	1.21
KELT-3b	9.8	0.0098	197	2.7

Exoplanet observation procedures were developed similar to the beta observation procedure for the Faroe Islands utilizing FireCapture image acquisition software, see Penn et al., 2015 [25]. Procedures aim to make data collection standardized so observations of the same target by multiple teams can be easily compared and combined for more accurate curve fitting. A standardized observation worksheet based on the one developed by Dennis M. Conti available at astrodennis.com is being used for CATE exoplanet observations. Observers use the worksheet to record observation details such as target, location, time, imaging properties, and observing conditions. The worksheet follows the data collected into the data analysis phase where details of the analysis can be recorded for each analysis run. The worksheet becomes an important part of the record keeping on producing light curves using different analysis parameters from the original data set.

Table 2.2. HD209458b observable transits July 15, 2018 through December 3, 2018 for Illinois and Oregon. Data from the Exoplanet Transit Database [30].

HD209458b		
Tmid (HJD)	Begin UT (mm/dd/yy hh:mm)	End UT (mm/dd/yy hh:mm)
2458314.662	07/15/2018 2:21	07/15/2018 5:25
2458321.712	07/22/2018 3:32	07/22/2018 6:36
2458328.761	07/29/2018 4:43	07/29/2018 7:48
2458335.811	08/05/2018 5:55	08/05/2018 8:59
2458342.86	08/12/2018 7:06	08/12/2018 10:10
2458374.583	09/13/2018 0:27	09/13/2018 3:31
2458381.632	09/20/2018 1:38	09/20/2018 4:42
2458388.682	09/27/2018 2:49	09/27/2018 5:53
2458395.731	10/04/2018 4:00	10/04/2018 7:05
2458434.504	11/11/2018 22:32	11/12/2018 1:37
2458441.553	11/18/2018 23:44	11/19/2018 2:48
2458448.603	11/26/2018 0:55	11/26/2018 3:59
2458455.652	12/03/2018 2:06	12/03/2018 5:11

The Citizen CATE telescope setup is portable and so each observation session starts with equipment being setup and the mount being aligned. A great deal of time can be saved in this step if observers perform the polar alignment on an earlier evening. The scope can be left in place or the positions of the scope legs can be marked on the ground and returned to the same position. Camera equipment and the computer is connected to the telescope during setup to allow adequate warm-up time of at least 20 minutes for the camera. Up to two hours temperature stabilization may be required for the scope to reach equilibrium with the outdoor temperature and clear condensation from the optics. Time on the computer should be set to 24 hour display and synchronized. FireCapture [12]

software on the laptop and allows the user to monitor camera temperature and observe stability. In FireCapture the user needs to then verify the correct settings for image capture, and take a test frame. All observations use File Image Transport System (FITS) image files in 16 bit format. Zero camera gain is used to minimize noise. Exposure is set to the lowest possible exposure at this point to be able to see stars in the field of view and focus the telescope. The focus should be adjusted so that stars appear as round points of light. A test image should be taken and examined using a FITS file reader or AstroImageJ. The observer should examine the FITS header to make certain the image properties listed in the FITS header match intended settings. The time recorded in the FITS header DATE-OBS field should match the current universal date and time. Discrepancies in the time should be noted on the data sheet.

The FITS file format has been chosen because it is a standard astronomy file format that can be shared between groups, and it is the required format for analysis in AstroImageJ, the software package that is used for data reduction and light curve plotting. AstroImageJ pulls the time information for light curve plots from the FITS header DATE-OBS field. In test observations, problems arose after data had been collected due to computers recording the time in unexpected ways. Although time was set to 24 hour format on all observation computers, times recorded in FireCapture [12] would sometimes show as AM / PM, and then be converted improperly to UT time when the DATE-OBS field was created. Furthermore, daylight savings time considerations and computers having the wrong time zone selected caused problems with the recorded times being off by hours. Time issues that came up could be corrected prior to model fitting and light curve plotting although utilizing GPS for a standardized time as done for the CATE solar project would be a better solution.

2.3.1 Calibration Images

Calibration images consisting of field flats, bias frames, and dark frames can be used to reduce noise in the data images. While these will be required when looking at dim or

low depth transits, they were not used for this initial observation of bright transits.

2.3.2 Test Images

The telescope should be pointed such that the target star is centered in the field of view. Tracking on the scope should be turned on at this time, and guidance if used. Ten test images of the star field should be taken in FireCapture [12] by setting up a short data acquisition run using the same parameters to be used in the full data acquisition. One of the images should be plate solved using software on the local computer from Astrometry.net [19] to verify the target. The telescope should remain on target and any alignment or tracking adjustments should continue to be made until it is time to start taking transit data.

2.3.3 Data Storage Considerations and Acquisition

FireCapture allows an automated data run to be setup to take any number of images at predetermined exposures [12]. This allows the images to be captured and saved automatically for the duration of the observation. Images should be captured for the length of the transit plus one hour. Data acquisition should start 30 minutes prior to the transit and continue for 30 minutes after. A delay of 3 to 10 seconds should be set between exposures. The delay results in less data being collected to save on storage space, and it also helps to lower noise in captured images. The user must insure that enough storage space is on the computer prior to capturing data. Space required assuming 16Bit FITS files at $\approx 10\text{MB}$ each is calculated as follows where S = amount of space, t = time of data acquisition, and r = frame rate, $S = t * r * 10\text{MB}$. The amount of storage space needed for a short (2 hour) transit using a 2 second exposure and a 3 second delay would be $\approx 22\text{GB}$.

During data acquisition, the observer needs to monitor progress to make sure files are being written to the proper directory on the laptop. Any significant image drift should be corrected by moving the telescope back on target to keep the target star centered as well

as potential comparison stars in the field of view. Following the observation a backup of the data should be performed to an external storage device as soon as possible.

2.4 DATA COLLECTION AND REDUCTION

Data was collected on HD209458 (Elmore, Cobble, Baer, Conley) and HD189733 (Baer and Conley). Analysis of the most complete and cleanest data for HD20948b and HD189733b observations by CATE volunteer Conley are presented.

2.4.1 HD209458b Observation

A transit of HD209458b was observed on October 11, 2018 by CATE volunteer Mike Conley of Salem Oregon. Conley recorded data from 11 October 2018 4:41:44 UT to 11 October 2018 8:50:12UT. The transit was predicted to occur between 5:12UT and 8:16UT with an expected midpoint at 6:44UT. Weather for the observation was clear. Conley used the CATE scope attached to a Celestron AVX GoTo mount with PHD2 guiding software running on the CATE laptop. 2,474 FITS 16 bit image files were captured with 2 second exposure time, zero camera gain, and a delay of 3 seconds between exposures for the duration of the transit plus 30 minutes before and after.

2.4.2 HD189733b Observation

Observation of HD189733b was carried out by Mike Conley in Salem Oregon on October 12, 2018 utilizing the standard Citizen CATE setup with the addition of the Z-field dual axis CG4 controller for pointing and computer assisted manual guidance functions. The transit was predicted to occur between 5:25UT and 7:15UT with an expected midpoint at 6:20UT. Weather during the observation was clear. 1,554, 16 bit FITS images were taken using 2 second exposure, a 3 second delay, and zero camera gain from 30 minutes before the expected transit to 30 minutes after.

2.4.3 Data Reduction

Prior to photometry analysis, bad images were removed from the data set. In the analysis of HD209458b, six frames were discarded that showed signs of excessive mount movement, shifting of the star field, or streaks indicating a satellite or meteor passing close to the region of the target or comparison stars as shown in figures 2.2 and 2.3. Unremoved light streaks over the comparison or target stars will create excessive noise in the data set by contributing to the flux calculation of stars.



Figure 2.2. HD209485b discarded frame showing excessive mount movement. Stars appear as horizontal smears across the sky instead of well defined points of light.

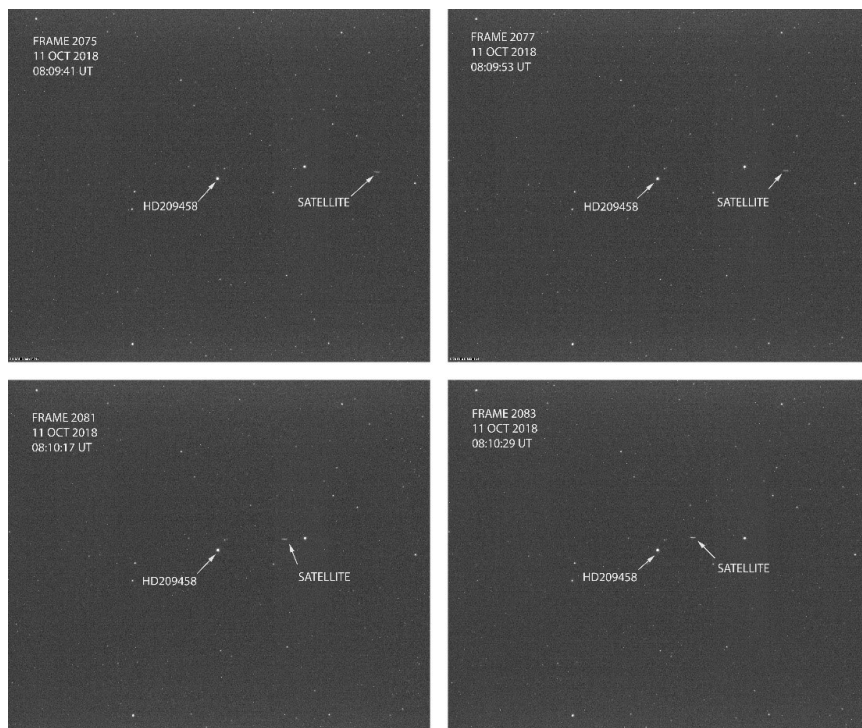


Figure 2.3. HD209458b frames showing satellite in FOV

The FITS headers of each remaining file was modified in AstroImageJ [9] to add the Julian date to each file header. The Julian date is defined as the time elapsed in days from Jan 1, 4713BC Greenwich noon time. Julian date for October 11, 2018 at the predicted transit start, 05:12 UT is: 2458402.71667. Modification of the FITS header was done using automated tools in AstroImageJ. Care had to be taken to verify the timestamps in the FITS header used as input for AstroImageJ were correct. After the FITS header was updated, photometry analysis could be done on the files in AstroImageJ. This was accomplished by calculating the relative flux of target and comparison stars. First, the flux of each star had to be determined by comparing the light within a circular area to the background light. This was done by setting a series of apertures with radii that maximized the signal of the target star relative to the background level. The innermost aperture contains pixels that are used to calculate the total source flux while the outermost aperture defines the background flux.

The radius of the apertures on the target and comparison stars is determined to maximize the signal to noise ratio between the source and the background. AstroImageJ [9] includes a radial profile (seeing profile) plot tool that assists the user in determining the appropriate sized source and background radius. The tool displays the half width at half maximum, full width at full maximum, and suggested radii of apertures in pixels [9]. Once the appropriate aperture size is determined, apertures for comparison stars can be placed in AstroImageJ. The measured flux of each star is calculated by summing the source values of each pixel in the source aperture and subtracting the background value.



Figure 2.4. Aperture placement in AstroImageJ. The source aperture is defined by the innermost circle. Background aperture is defined as the region between the outermost and the middle circle.

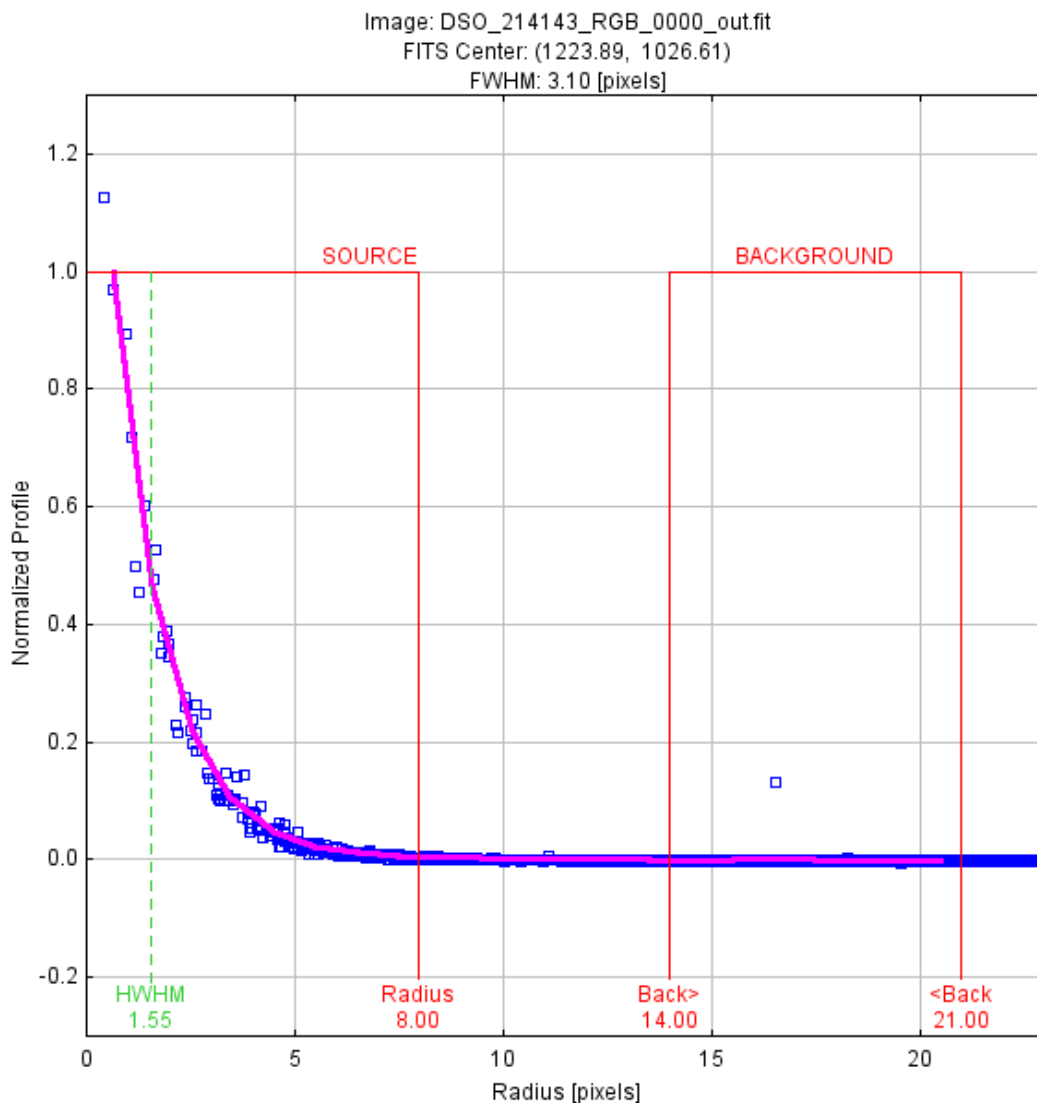


Figure 2.5. AstroImageJ seeing profile of HD209458b. Aperture settings tool displays suggested source and background annulus of 8, 14, and 21 pixels.

Relative flux of the target star, F is then calculated by dividing the measured flux of the target star, F_T by the summation of the measured flux of n comparison stars F_C . [9]

$$F = \frac{F_T}{\sum_{i=1}^n F_{C_i}} \quad (2.1)$$

The relative flux, F , of a comparison star C_j is calculated as shown below:

$$F = \frac{F_{C_j}}{\sum_{i=1}^n F_{C_i}}, i \neq j \quad (2.2)$$

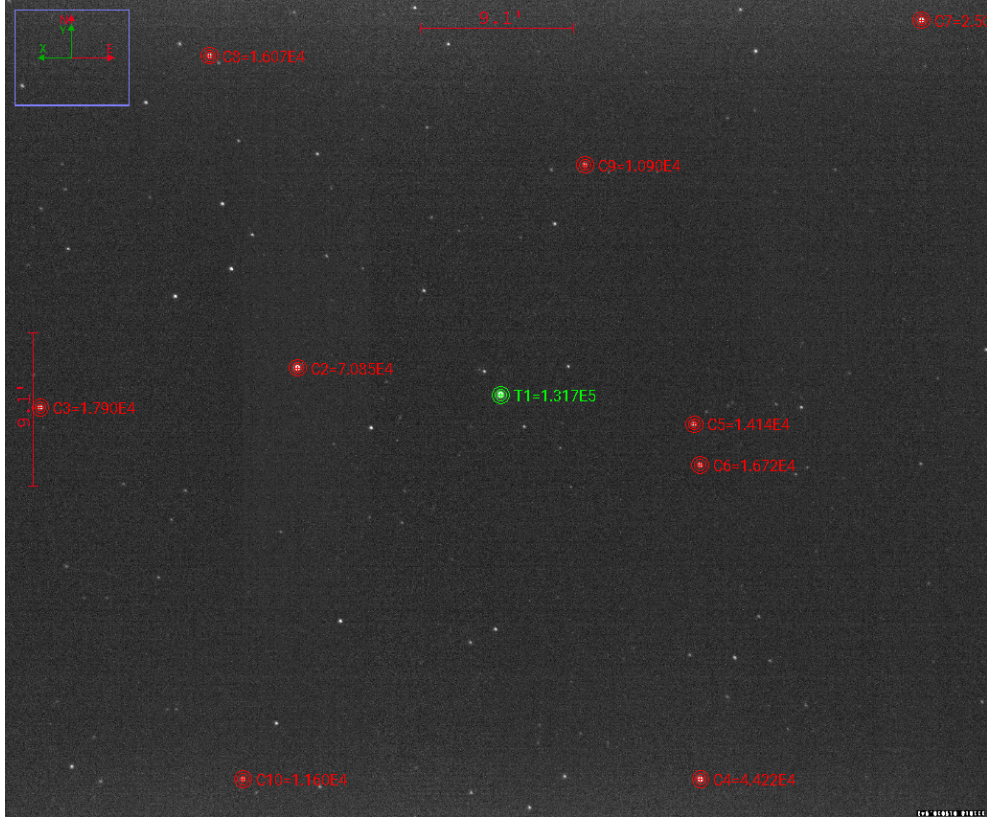


Figure 2.6. HD209458 source and comparison stars. Target star (T1) shown in green. Comparison stars C2 thru C10 are shown in red. Numerical values are the calculated fluxes of each star.

Values for the relative fluxes, observation time, location information, and several optional parameters are output from AstroImageJ [9] into a comma separated value measurements file. Further analysis is carried out on the measurements file and images from the observation are generally no longer needed. This results in a significant data reduction from the original 2474, 10MB image files that took up 24GB of storage space to a single file taking up 5MB of storage space. This type of data reduction will become important later in the project as volunteers accumulate large amounts of data on multiple transits. Storing the measurements file is easy to do whereas storing the original transit images becomes unrealistic with 72 sites accumulating on the order of 25GB each per transit observation. The observation network would generate just under 2TB of image data per target.

Relative flux of the host star HD209458 was calculated compared to 9 comparison stars. Comparison stars are ideally chosen as stars in the FOV with brightness similar in magnitude of target star. For HD209458, most of the comparison stars were considerably lower magnitude ($V=9$ to 11 magnitude) than the host star ($V=7.65$ magnitude). Images were well aligned from one to the next with little drift. Out of the original 2,474 image files, 2,468 were used for plotting the light curve.

2.4.4 Noise Reduction

A significant source of noise in the images can be from hot and dark pixels in the image sensor. These pixels will always be either too bright or too dark and can contribute to noisy data. Image shifting due to tracking errors can make the noise of these hot and dark pixels more noticeable. Throughout the observation, the image shifts slightly due to imperfect tracking and guiding on the mount. Image shift for observations of HD209458 was up to 14 pixels in the X direction and 37 pixels in the Y direction over the length of the entire observation while image shift from one successive image to the next was much lower, never exceeding more than a few pixels in either direction.

Calibration of images becomes important when trying to detect shallow transits. Successful detection of transits with depths of 1% or less typically requires images to be calibrated with a series of additional images taken during observations [4]. Calibration images can include dark frames, flat field frames, and bias frames. The inclusion of these calibration images in the image processing typically results in cleaner images that take into account imperfections in the camera and optical system. The transits observed in this project were of significant brightness and relatively high depth that did not require such calibration to be observable.

AstroImageJ has a feature that attempts to remove hot and cold pixels (outliers) that have values falling outside of expected range for neighboring pixels. This can remove bad pixels as well as streaks in the images and replace the removed pixels with an average neighboring pixel value. In some instances, removing outliers in AstroImageJ may cause a

significant noise reduction thus improving the accuracy of the light curve, however it could result in data degradation [9].

Figure 2.7 shows the contribution of hot pixels to the source and background flux. Hot pixel 1 contributes to the background in frame 1, but not in frame 59 thereby reducing the background flux level as the image shifts from frame 1 to 59. Hot pixel 2 is outside of all apertures in frame 2, but in the source aperture in frame 59 resulting in an increase in the source flux calculation. The image shifting can lead to noise in the data. Removing hot pixels from the images can reduce the noise in the flux measurement. The process of removing outliers in AstroImageJ creates another set of images with the outliers removed that measurements can be run on. This was done for both data so the results of measurements with and without outliers removed could be compared in each case. If removing outliers can significantly improve the measurements, this process could result in lower observable transit depths without the need to take image calibration data.

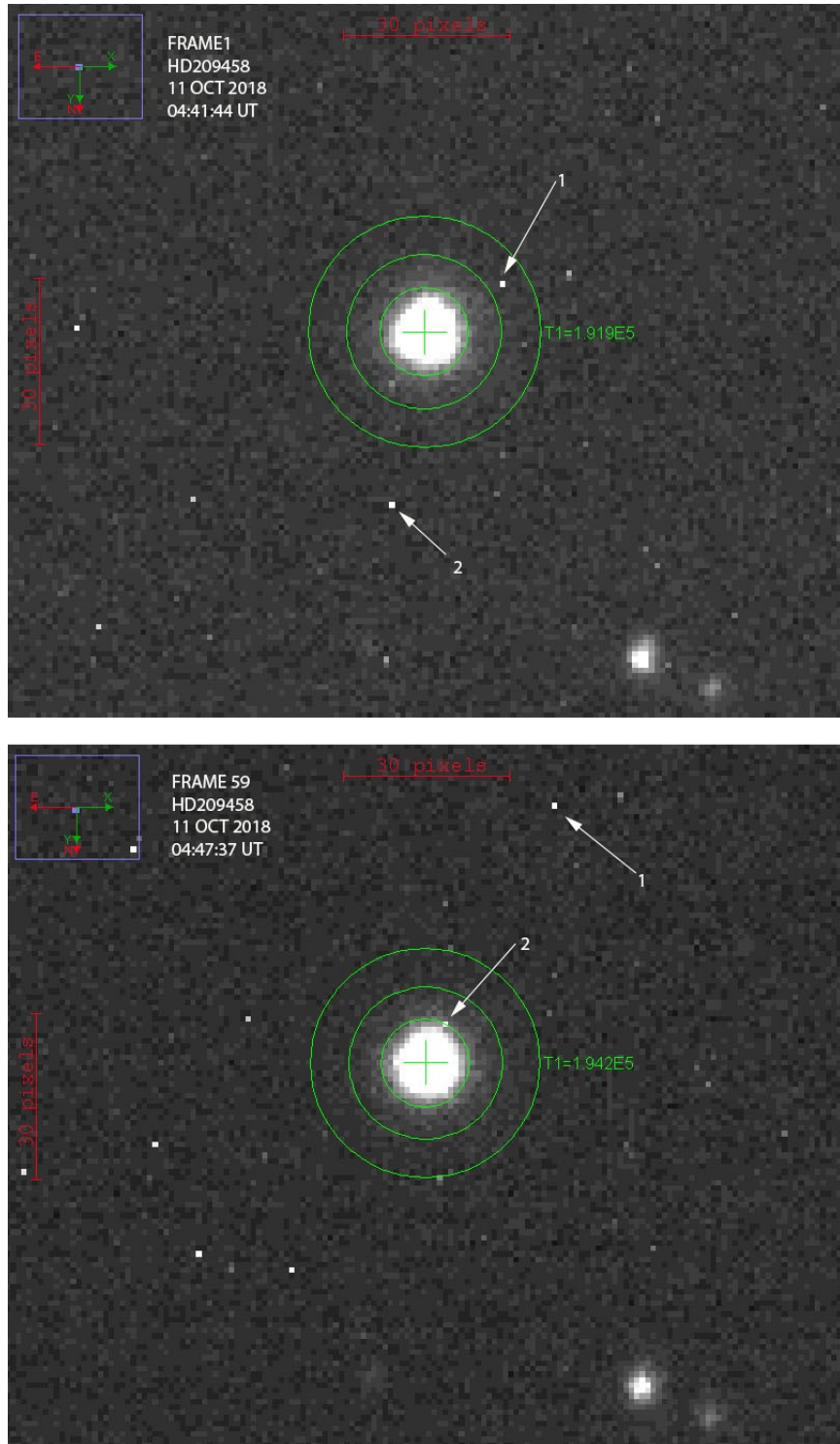


Figure 2.7. Shifting of hot pixels relative to target star demonstrated from frame 1 to frame 59 of HD209458b. Arrows indicate selected individual pixel locations in each frame.

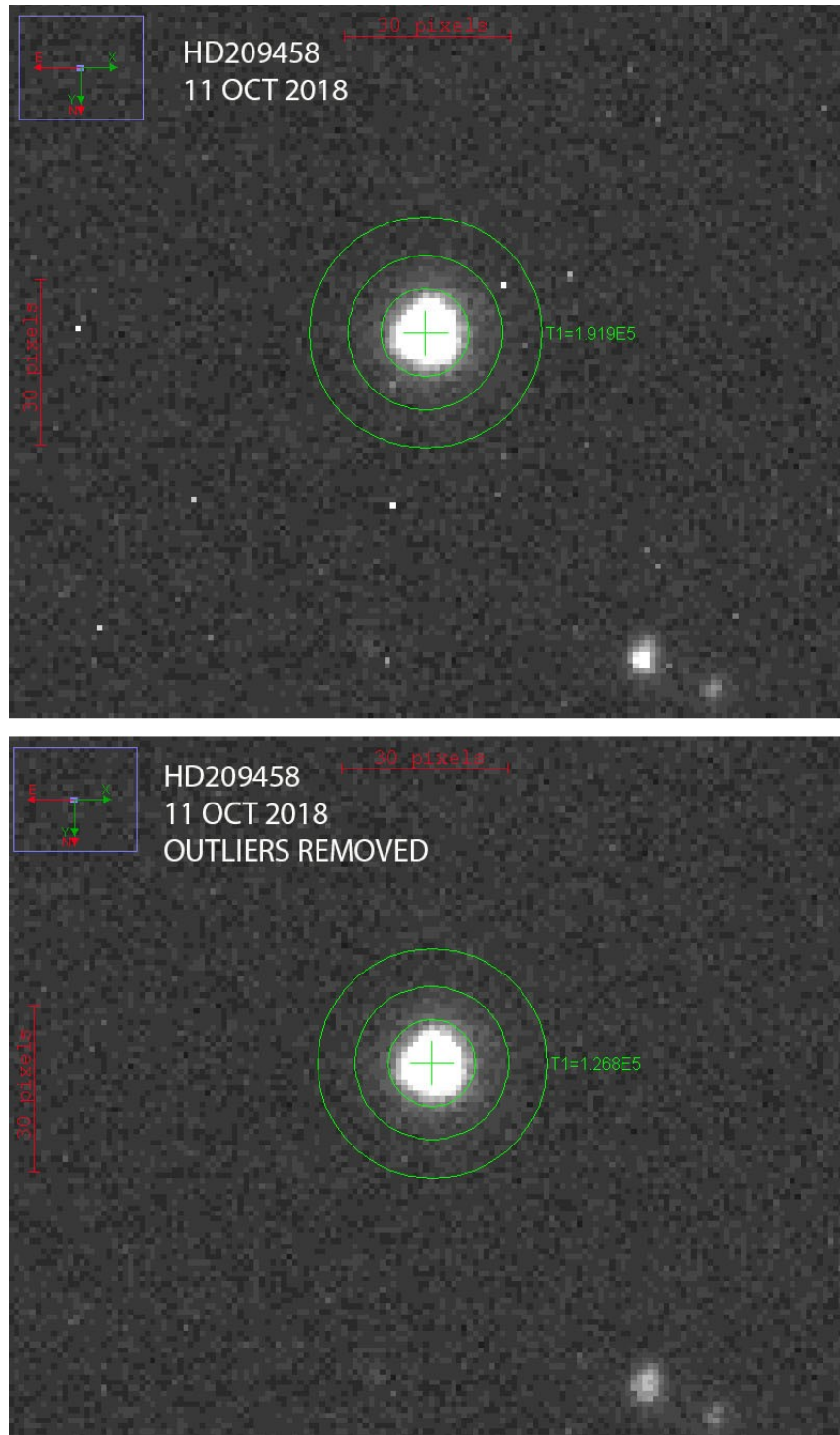


Figure 2.8. HD209458b original data (top image) vs outliers removed (bottom image).

CHAPTER 3

ANALYSIS

3.1 TRANSIT MODEL FITTING

The Light curve model fitting in AstroImageJ [9] uses the small planet approximation described by Mandel and Agol, 2002 [20]. Model fitting assumes a transit fit for the host star and linear fits for the comparison stars. Model fitting and plotting is described in further detail by Collins et al., (2017) [9]. The most accurate results will be obtained when known or suspected parameters for the host star and orbital parameters of the exoplanet are input to AstroImageJ. Current values for HD209458b and HD189733b orbital parameters and host star effective temperature were obtained from the NASA Exoplanet Archive [22], or Exoplanets.org [14]. A table of the published host star and planetary transit data is shown in table 3.1.

AstroimageJ [9] plots the relative fluxes of the host and comparison stars from data in the measurements file. It can also perform the light curve fitting on the fly or at any time after the plot is done. Curve fits are made more accurate by inputting known planet orbital parameters such as the period, eccentricity, and argument of periapsis ω . AstroImageJ automatically calculates all parameters needed on the host star from a single user provided parameter. For all calculations, the effective temperature of the host star was used. The inclination of the planets orbit was well known for each planet and locked in all calculations. Quadratic limb darkening coefficients as described by Mandel and Agol, (2002) [20] can be calculated using computer code as described by Eastmen et al., (2013) [11]. The code takes into account properties of the imaging system including specific optical filters used by previous transit observation campaigns. No filters were used in observations by Conley. An initial value of .3 was picked for each quadratic limb darkening coefficient and allowed to drift forming a best fit. This value was initially picked due to it being close to values used for similar visual systems. It was kept the same in all calculations for consistency. More accurate light curves will be possible in future

observations by using standard transit observation filters and accurate calculation of the limb darkening coefficients.

Table 3.1.

Transit and Host Star Parameters		
Value	HD209458b	HD189733b
Host star magnitude (V)	7.65	7.67
Transit Depth (%)	$1.5 \pm .0024$ [32]	$2.4 \pm .0058$ [32]
Duration (min)	184.2 [30]	109.6 [30]
Planet Radius (R_{Jup})	$1.39 \pm .02$ [30]	$1.13 \pm .01$ [32]
R_p/R_*	$.143 \pm .002$ [32]	$.116 \pm .001$ [32]
Transit Period (min)	3.52472 [27]	2.2185 [17]
Transit Eccentricity Ecc	.0082 [10]	.0041 [33]
Host Star Teff (K)	6092 [18]	4875 [18]
Inclination (deg)	86.59 [29]	85.51 [33]
ω (deg)	43.8 [13]	90 [14]
Spectral Type	G0V [14]	K1- K2 [14]

3.1.1 HD209458b

Figure 3.1 shows the AstroImageJ curve fitting interface. User specified parameters are input and AstroImageJ performs calculations on the measurements file containing relative fluxes of the source and comparison stars. Once curve fitting is complete, AstroImageJ displays green boxes around all calculated parameters as shown in Figure 3.1 and outputs information on the fit statistics. While curve fitting is taking place a plot is made displaying user selected data that can include the relative flux of the target star, comparison stars, and the model curve fit as shown in figure 3.2. Comparison star data points in all plots have been binned by averaging the closest two data points for display purposes. Predicted ingress and egress lines for the start and end of the transit are

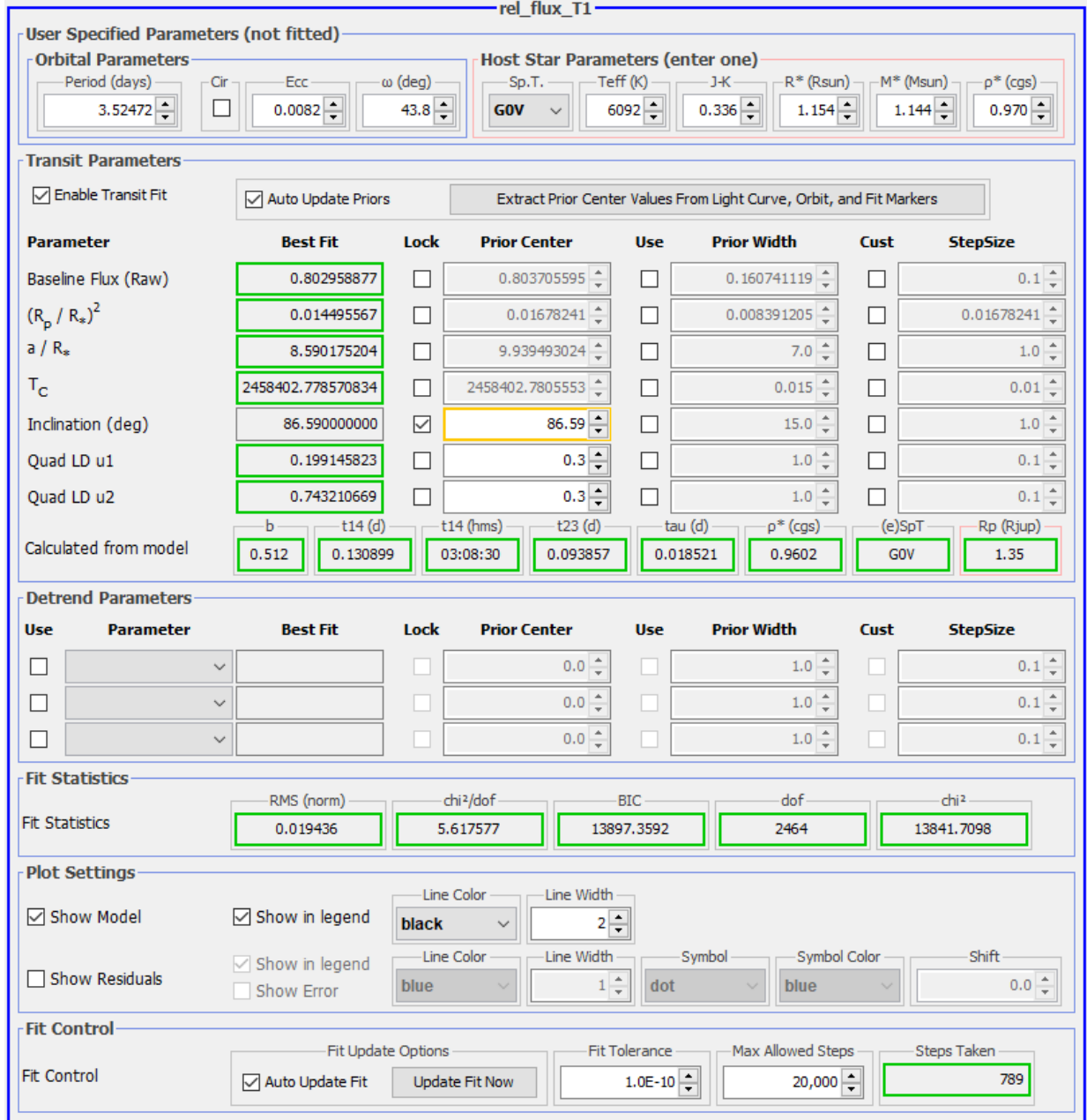


Figure 3.1. AstroImageJ curve model fitting of HD209458b. All comparison stars are used in this model fit.

displayed in red. In most calculations presented, the start and end of the transit for the curve fit is at the same point as the predicted start and end of the transit, although AstroImageJ does allow these points to be different as demonstrated in figure 3.8.

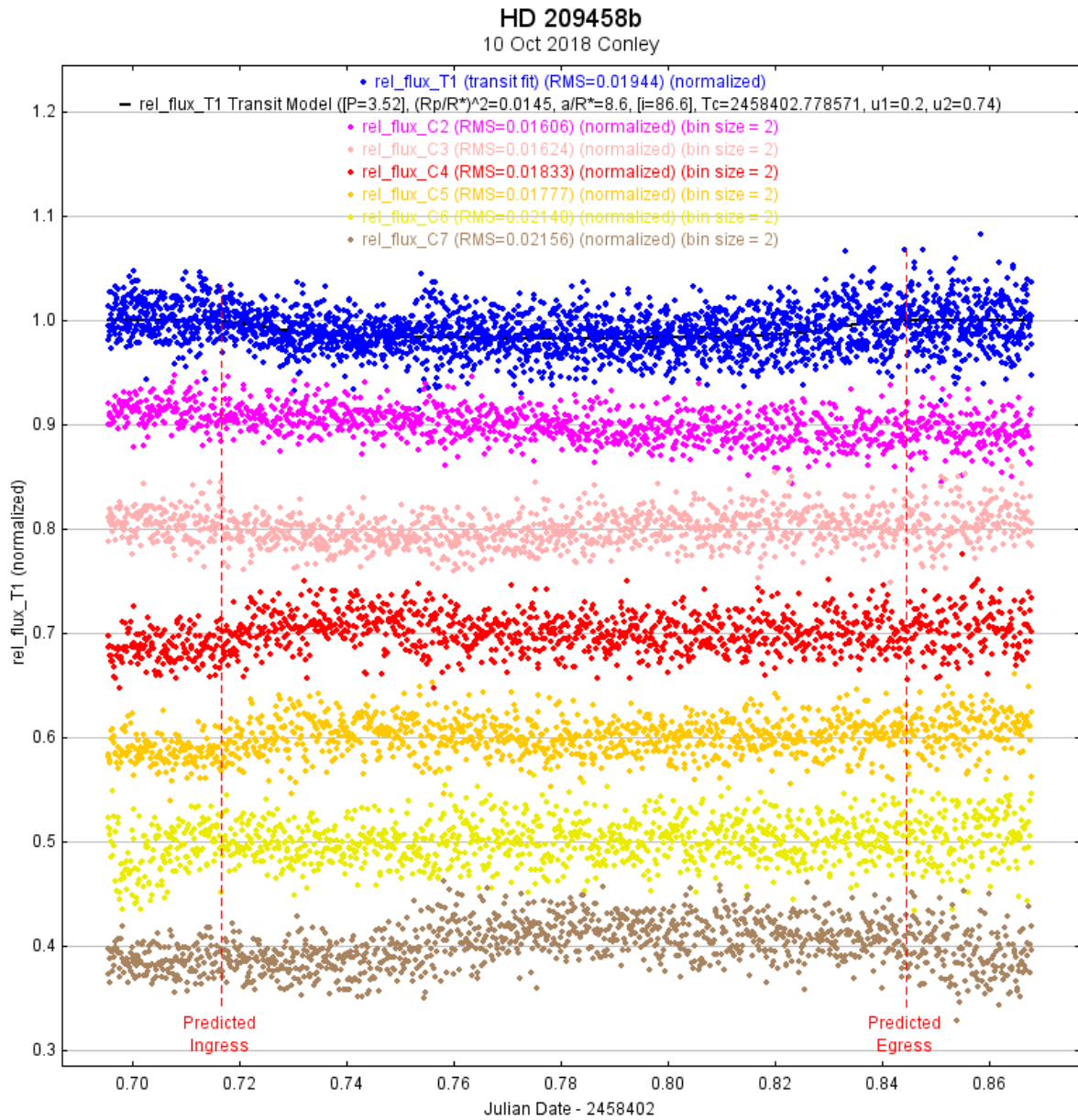


Figure 3.2. HD209458b transit light curve with 6 comparison stars shown. Black line represents transit model fit. Red vertical lines indicate the predicted start and end of the transit.

AstroImageJ [9] allows plots to be made showing any number of comparison stars, independent of the number of comparison stars used in the curve fit model. Figure 3.2 shows 6 out of the nine comparison stars while figure 3.3 shows no comparison stars.

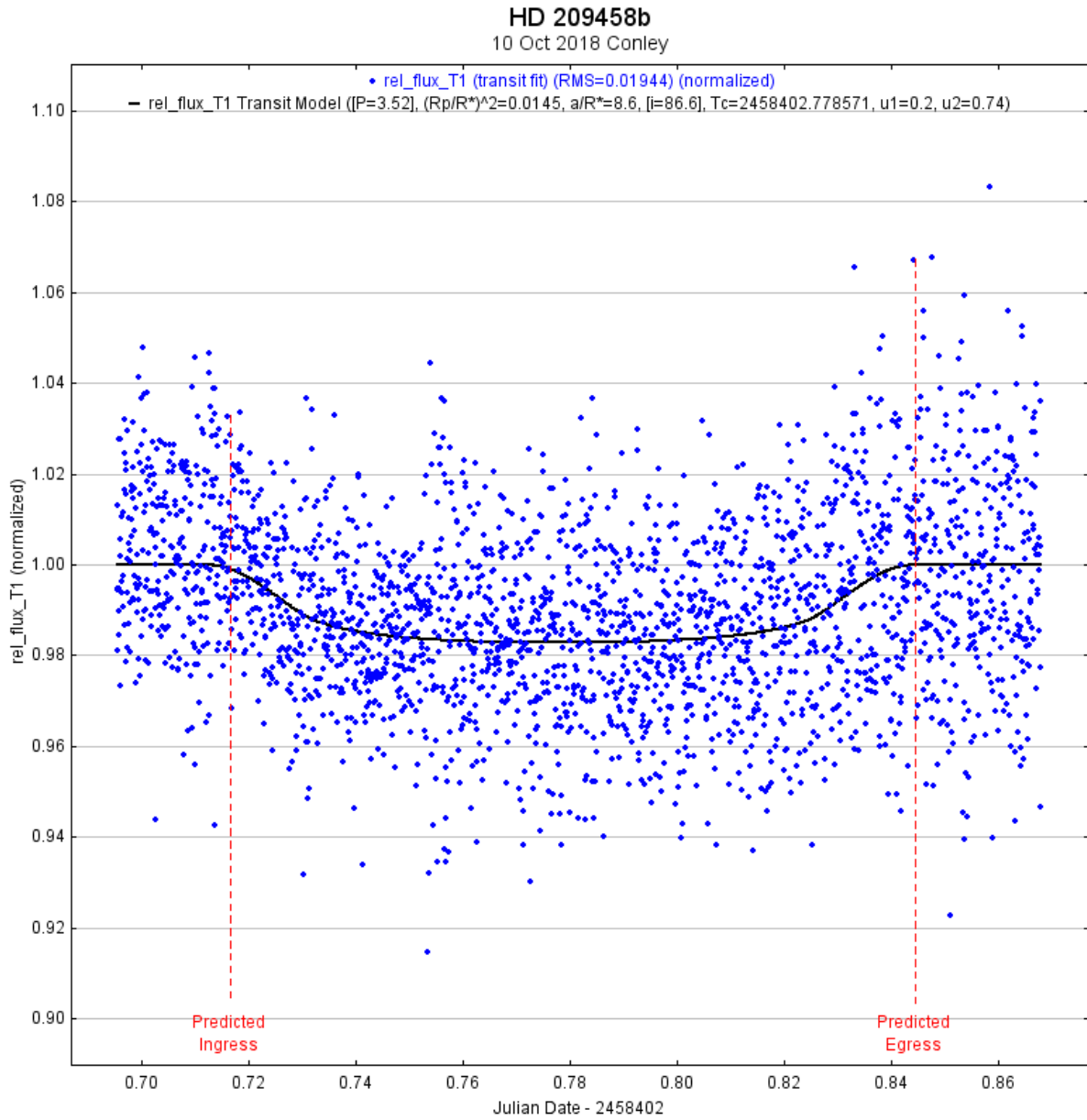


Figure 3.3. HD209458b light curve. Curve fit shows transit data is in close agreement with predicted transit start and end.

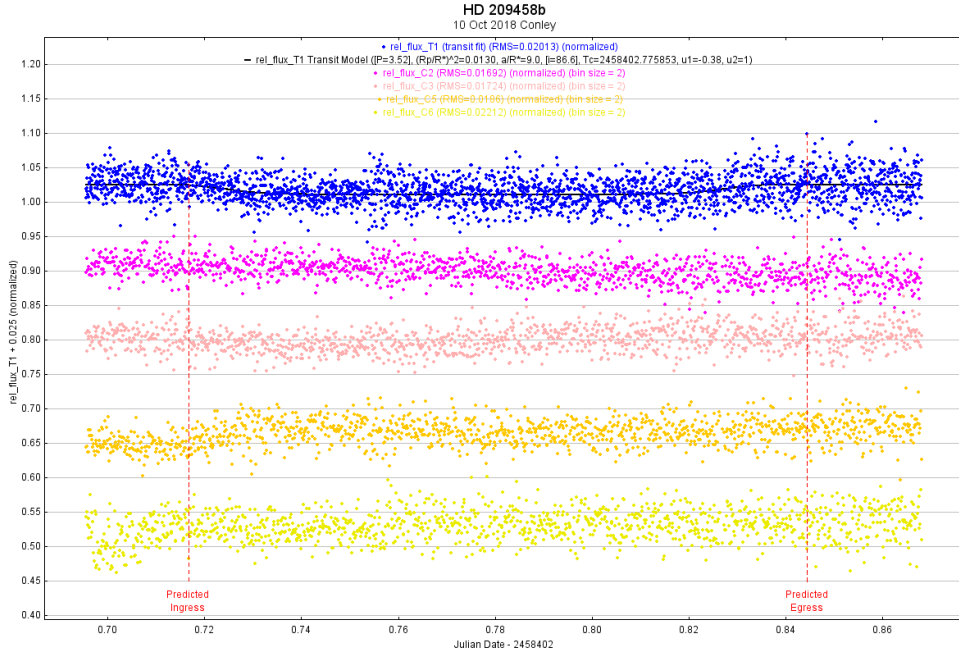


Figure 3.4. HD209458b light curve. Model fit uses the 4 most linear comparison stars

Calibration of the data was then done in AstroImageJ [9] to remove outliers from each frame. The resulting calibrated frames had considerably less observable noise in them than the original data. Comparing figures 3.11 and 3.13 it can be seen that several data values well outside of normal range have been removed, most notably toward the end of the transit. These out of range values were most likely due to rough movement in the mount as it tracked causing images of the stars to smear. The model fit shown in figures 3.4 and 3.5 was done using the 4 most linear comparison stars, dropping all other comparison stars from the model that appeared to have non-linear behavior. The observed radius of the planet calculated as $1.28 R_{Jup}$ is closer to accepted value of $1.39 R_{Jup}$, however the predicted egress is clearly further after the observed end of the transit than in early curve fitting using all comparison stars.

Further analysis of the HD209458b data was done by removing outliers from the observation images. The data was then replotted and curve fitting was performed to see if there was any obvious improvement in the data.

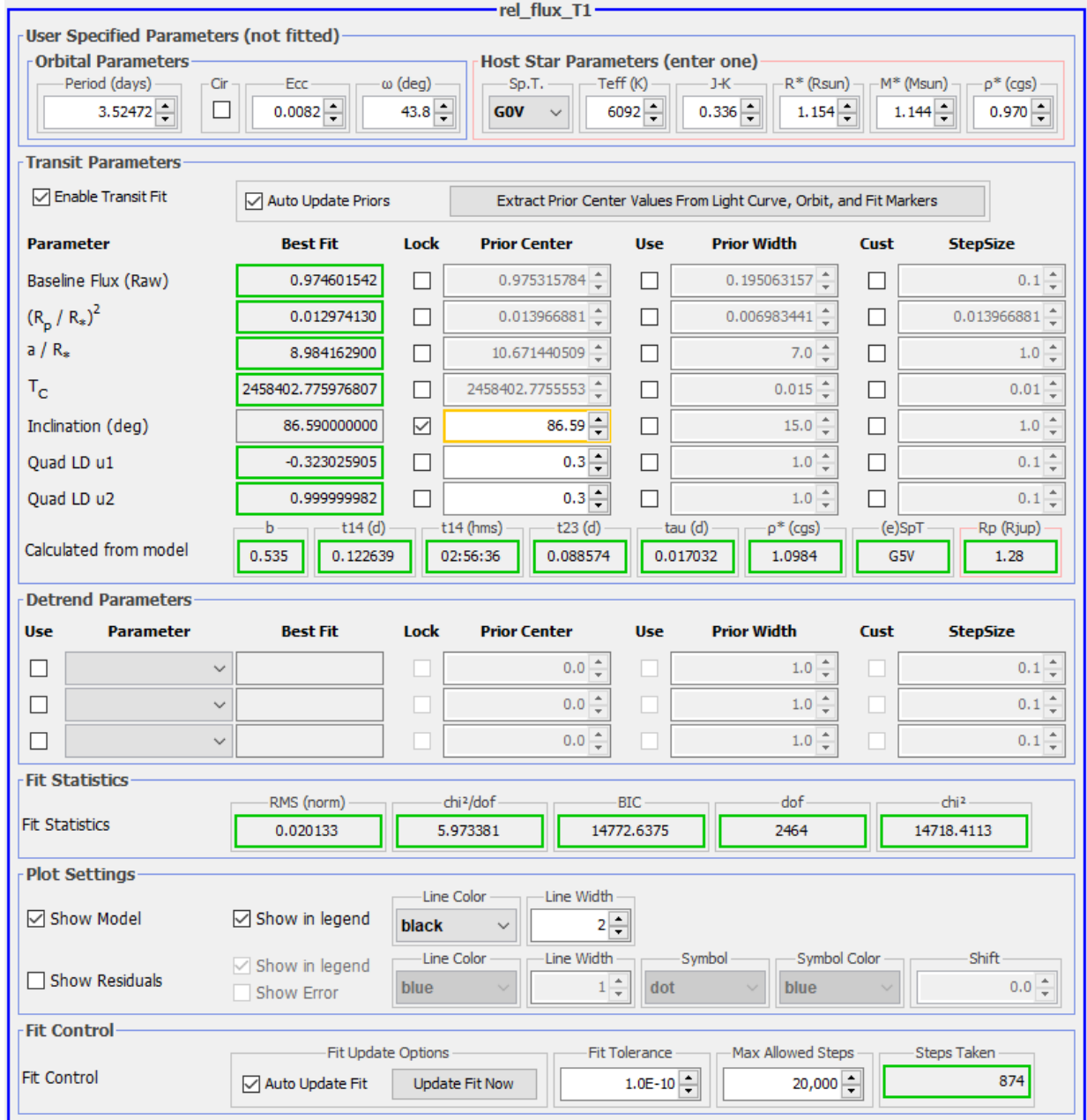


Figure 3.5. HD209458b model fit parameters using 4 most linear comparison stars.

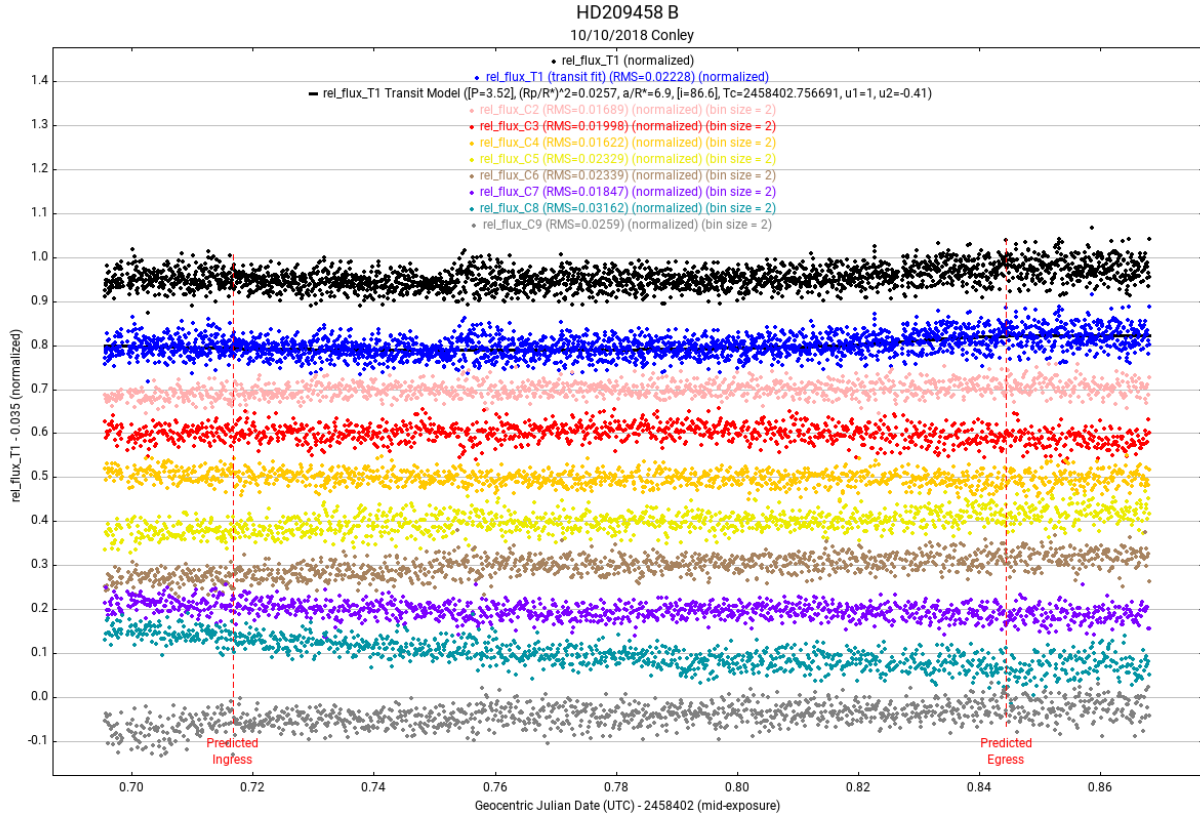


Figure 3.6. HD209458b light curve, outliers removed.

Removing outliers in the HD209458b data collected by Conley did cause slight changes in the transit parameters, however it does not appear that the results were significantly improved. It was also observed that removing outliers reduces the measured flux of the stars as can be seen in figure 2.8 by 1.92×10^5 to 1.28×10^5 or about 30%. Removing outliers in the data while making the data look slightly cleaner can reduce the signal to noise ratio in the overall data resulting in less accurate results.

Throughout analysis of HD209458 data, transit fits were done using nine, six, and four comparison stars. It was observed that only one of the nine comparison stars was well behaved, with the eight other stars showing varying degrees of nonlinearity and noise when plotted. This behavior is likely due to noise in the measurements that show up more in dimmer comparison stars due to the lower signal to noise ratio in their measurements. Including the maximum number of comparison stars in the measurements

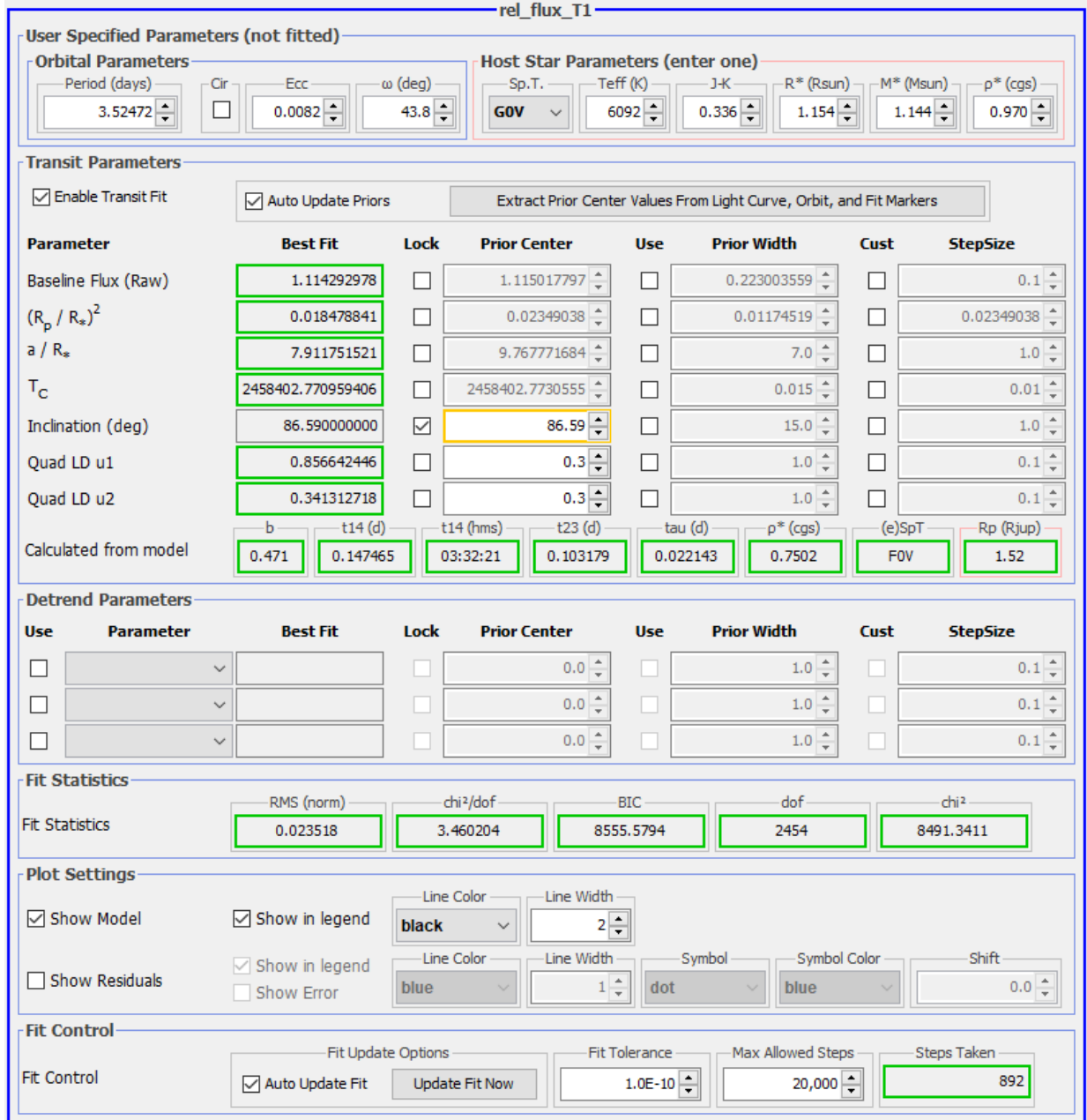


Figure 3.7. HD209458b model curve fit with 4 comparison stars used in model fit, outlier data removed. The duration of the transit is longer, 3:32:21, and the calculated size of the planet is larger $1.52R_{Jup}$.

has made the transit model fit parameters closer to expected values. It does appear that when the background is largely comprised of poor comparison stars, a more accurate model fit will be achieved when a large number of comparison stars is used.

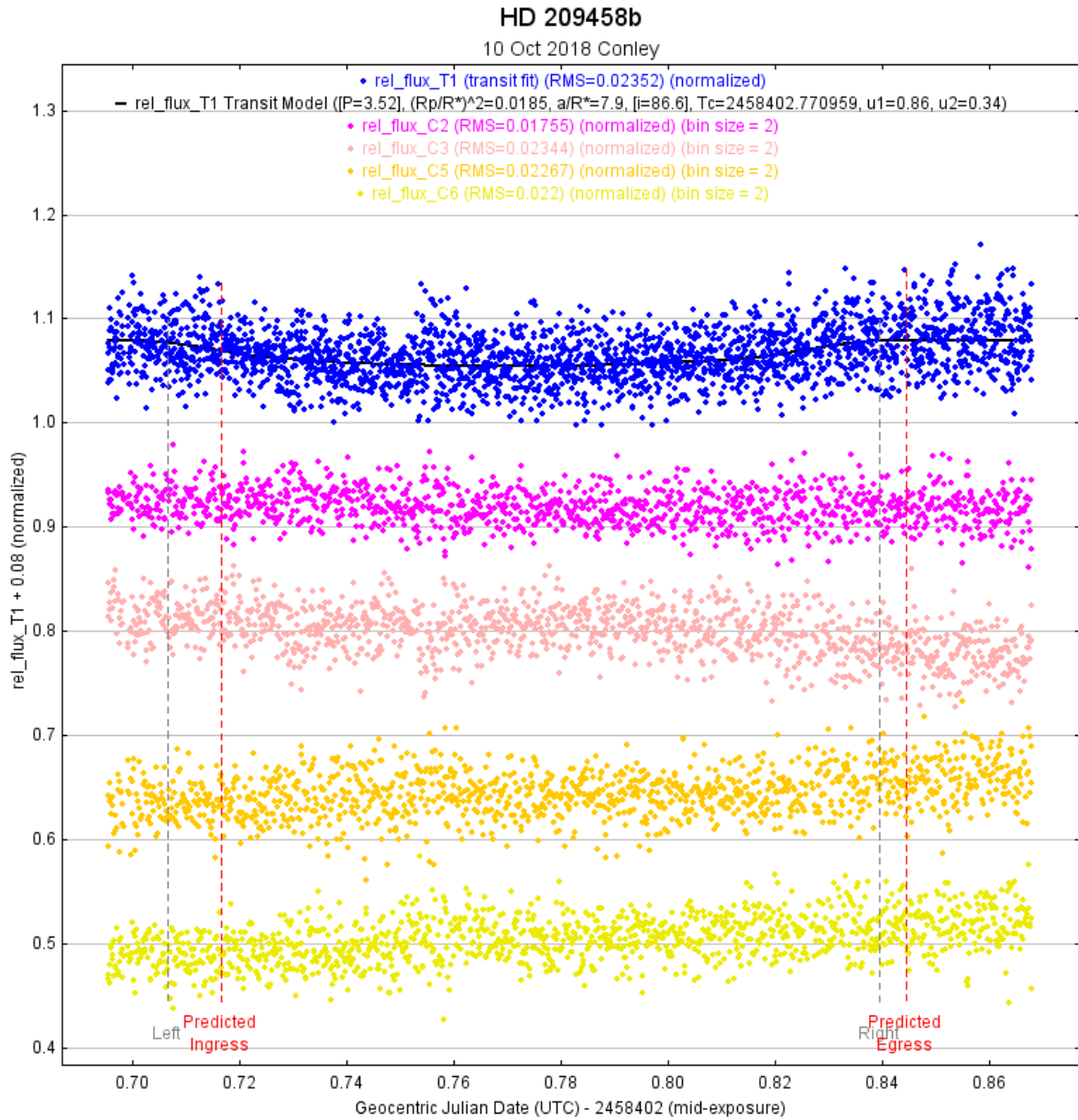


Figure 3.8. HD209458b light curve with four comparison stars, outlier data removed. Curve fit shows a data shift in the transit happening early and for a longer amount of time than predicted by ETD [30] published data.

Table 3.2.

HD209458b Measurements			
Value	Expected	Measured 5 Dec 2017	Measured 10 Oct 2018
Transit Depth (%)	$1.5 \pm .0024$ [32]	1.7	1.4
Transit Duration (min)	184.2 [30]	194.6	188.5
Transit Center (UT)	6:44 [30]	-	6:41
Planet Radius (R_{Jup})	$1.39 \pm .02$ [32]	1.54	1.35
R_p/R_*	$.143 \pm .002$ [32]	.132	.120

Table 3.2 shows the measured values from Dec 5, 2017 observations by Elmore, and Oct 10, 2018 observations by Coney using all comparison stars for the transit curve fit. Transit depth in each case is case is 1.7% and 1.4% respectively, which are very close to the depth of 1.5% measured by Stassun et al., 2017 [32]. Transit duration accepted value of 184.2 min was within 10 minutes of the duration observed by Elmore. Data did not include the first 20 minutes of the transit due to the transit starting before skies were dark enough to observe. The observation by Conley showed closer agreement, within 4 minutes of the accepted value. Time stamps on the data and FITS file headers came from the computer clock, which can be inherently inaccurate. For Citizen CATE solar observations, the timestamps were done using a GPS query [26], which will need to be utilized for later observations where the observation time will be known within a few seconds. The 4 minute difference in transit duration, and the 3 minute difference noted in the transit center could easily be explained by computer clock drift. The radius of the planet and the ratio of the planetary and stellar radius are in relatively good agreement with known values.

3.1.2 HD189733b

The relative flux of host star HD189733 and up to 8 comparison stars were plotted and used for transit model fitting. The brightness of comparison stars were general closer to the target star brightness than those used for HD209458 due to a larger number of suitable comparison stars in the FOV. Guidance of the telescope mount was sufficient to limit movement of the image to 15 pixels in the X direction and 29 pixels in the Y direction. While the total amount of shifting was similar to what was seen in HD209458 observations, large shifts of 15 pixels or more from one image to the next were a problem. This was caused by manual corrections in the telescope pointing to correct long term drift. AstroImageJ is not able to deal with image shifts of more than a few pixels from one frame to the next and so the measurements phase of the analysis failed initially. The images were plate solved in order to provide AstroImageJ a means of locating the target and comparison stars on each image.

Plate solving was done by installing a local copy of the Astrometry.net plate solving software on the observation laptop. This software runs in the background as a local web service. AstroImageJ [9] has the ability to submit plate solve jobs to the software locally, which saves a considerable amount of time over submitting them to an online plate solving service. Total time required to plate solve the 1,554 images was 8.5 hours, or about 3 frames per minutes. Once a frame is plate solved, the FITS header of the image is updated with World Coordinate System (WCS) information. This information contains pixel scale and location information for a reference pixel on each frame near the center of the image. From this information, the RA and DEC coordinates for each pixel can be calculated in AstroimageJ and used for image alignment. The center of each target and comparison star can then be located accurately from the RA and DEC information in the FITS header. In this way, the software can make up for relatively large shifts in the image.

The radius of the source and background annulus in AstroImageJ were chosen as 11, 20, and 30 pixels respectively. Eight comparison stars were selected for relative flux calculations. Several of the comparison stars ($V=8$ to 9 magnitude) were of similar

brightness to the target ($V = 7.67$ magnitude).

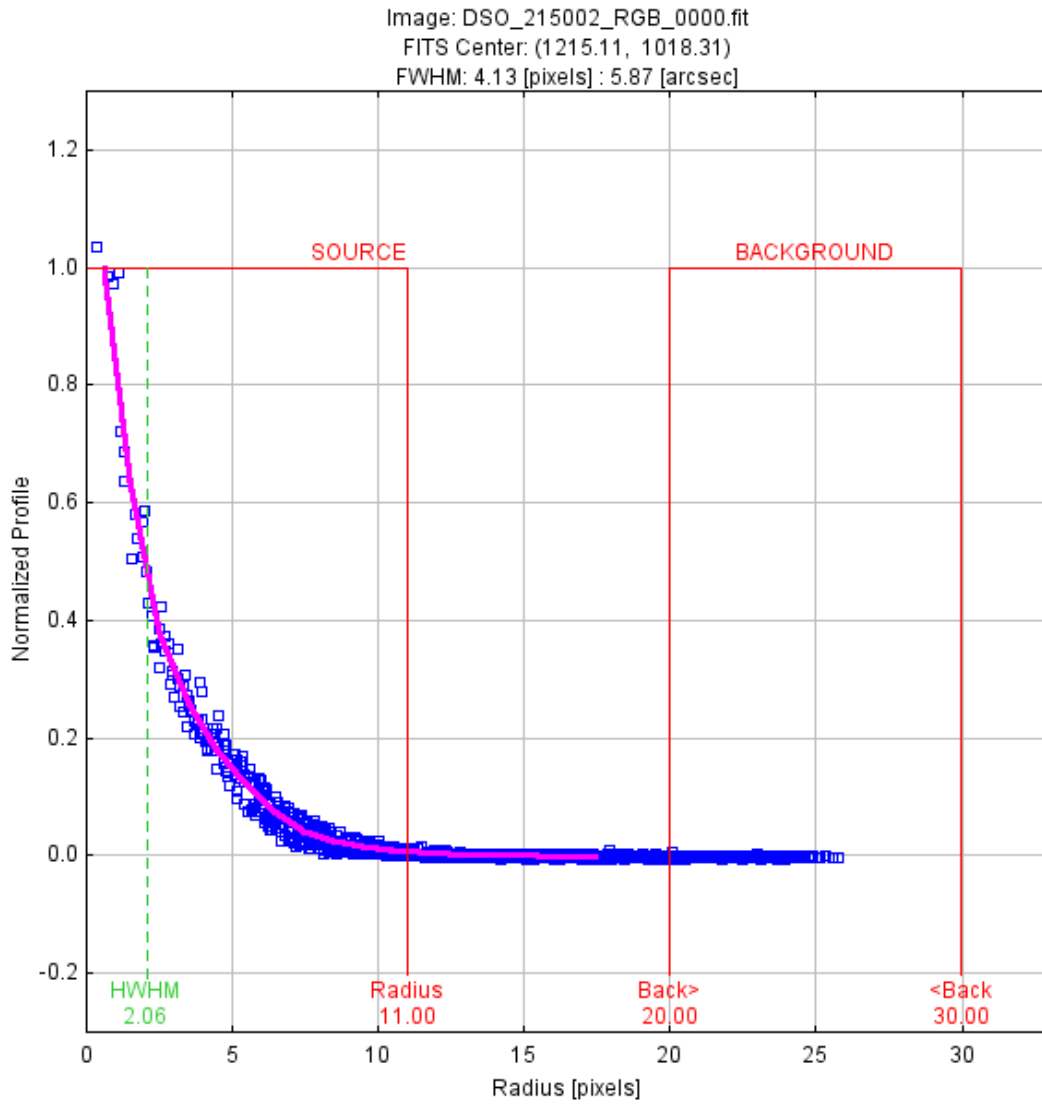


Figure 3.9. HD189733b seeing profile showing ideal radii for source and background apertures as well as full and half width half maximum relative flux values. Inner source radius is defined from zero to 11 pixel. Outer background radius is from 20 to 30 pixels.

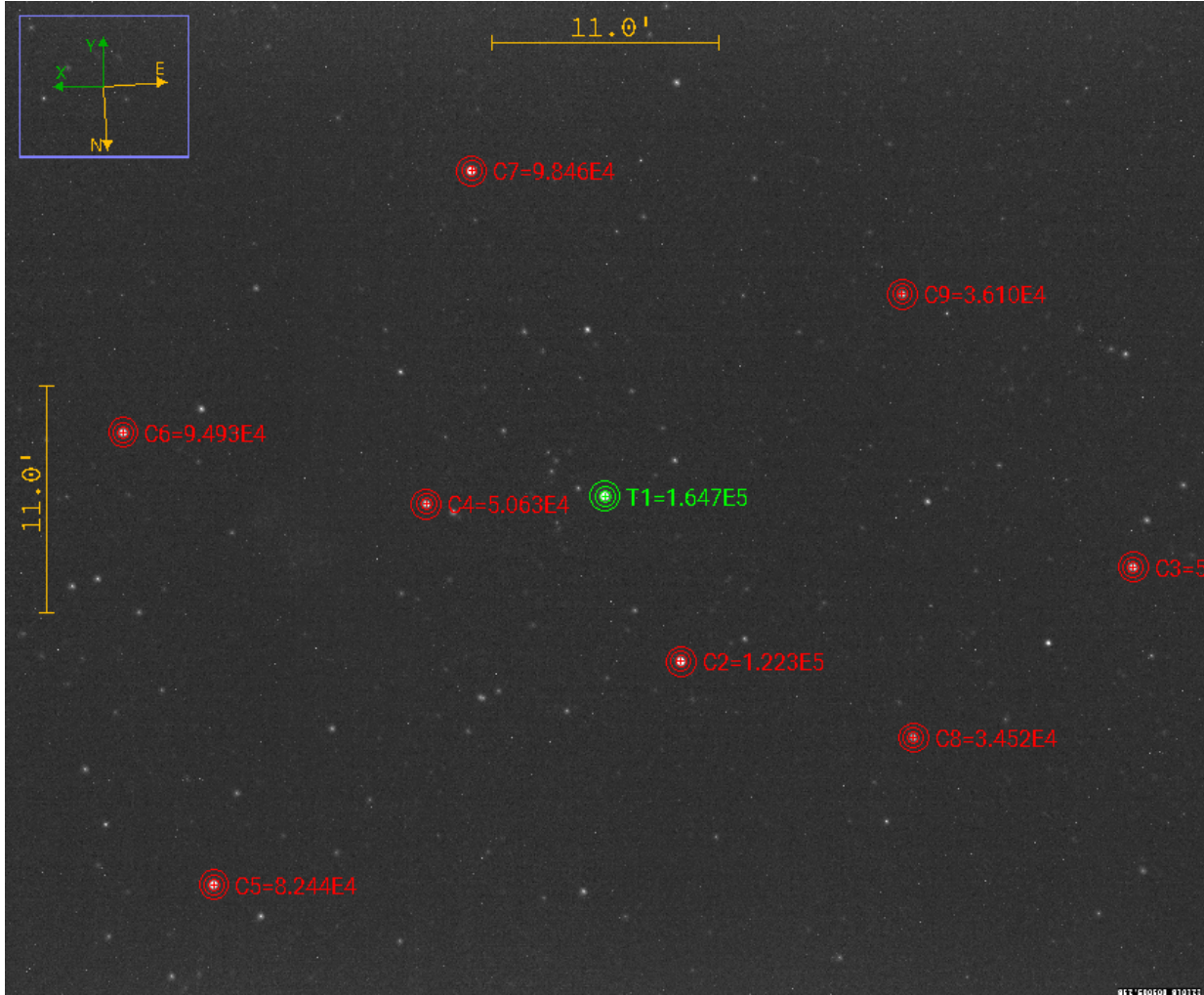


Figure 3.10. HD189733b target and comparison stars. Target star shown in green with 8 comparison stars shown in red. Measured flux values are displayed by target and comparison stars.

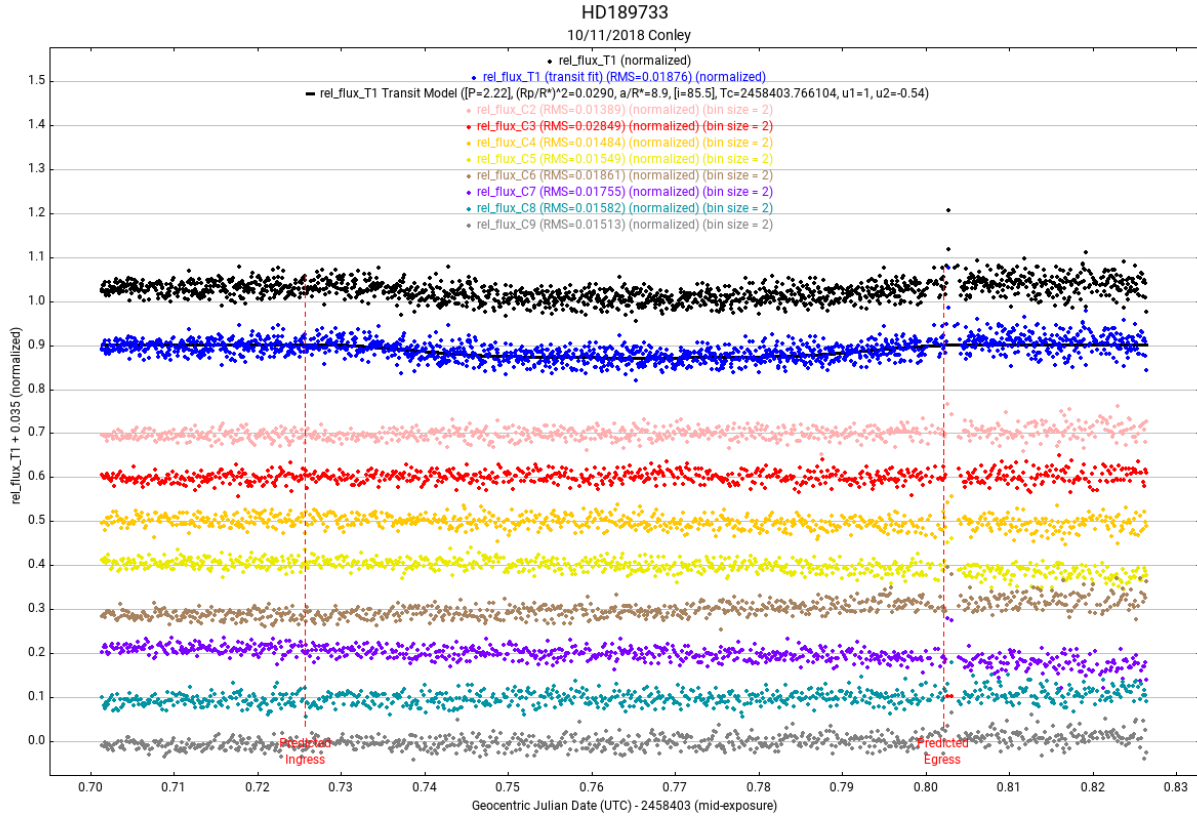


Figure 3.11. HD189733b light curve with 8 comparison stars. Black line indicates model curve fit.

HD189733 was plotted relative to 8 comparison stars of lesser magnitude. Values for the host star and orbital parameters from table 3.1 were used in the model fit. All comparison stars appear linear while the target stars curve fit appears to fit the predicted transit model well. There is visible noise in the data, especially toward the end of the transit. Initial fit parameters appeared reasonably close to expected values.

Calibration of the data was then done in AstroImageJ [9] to remove outliers from each frame. The resulting calibrated frames had considerably less observable noise in them than the original data. Comparing figures 3.11 and 3.13 it can be seen that several data values well outside of normal range have been removed, most notably toward the end of the transit. These out of range values were most likely due to rough movement in the mount as it tracked causing images of the stars to smear.

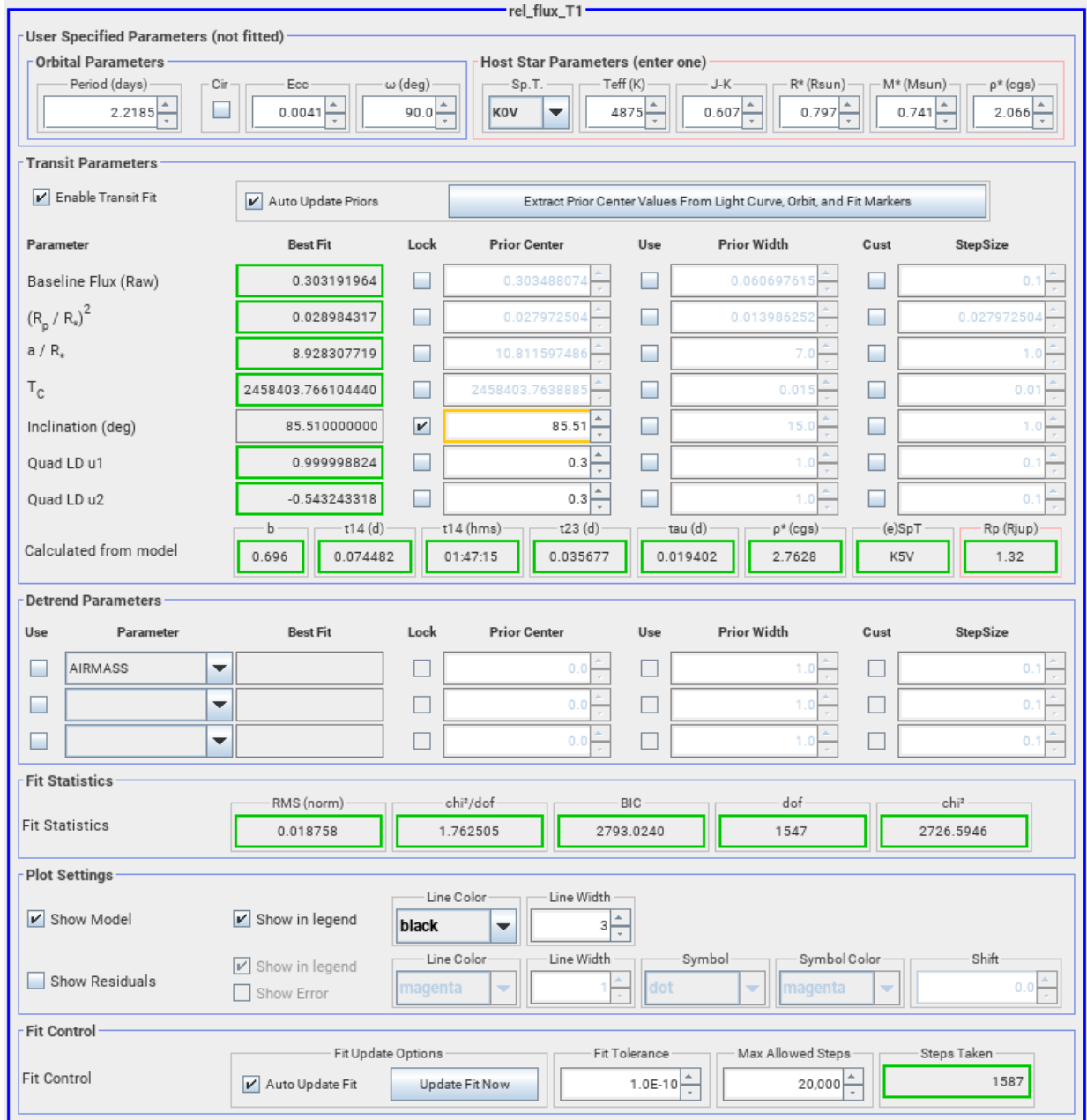


Figure 3.12. HD189733b model curve fit parameters using 8 comparison stars.

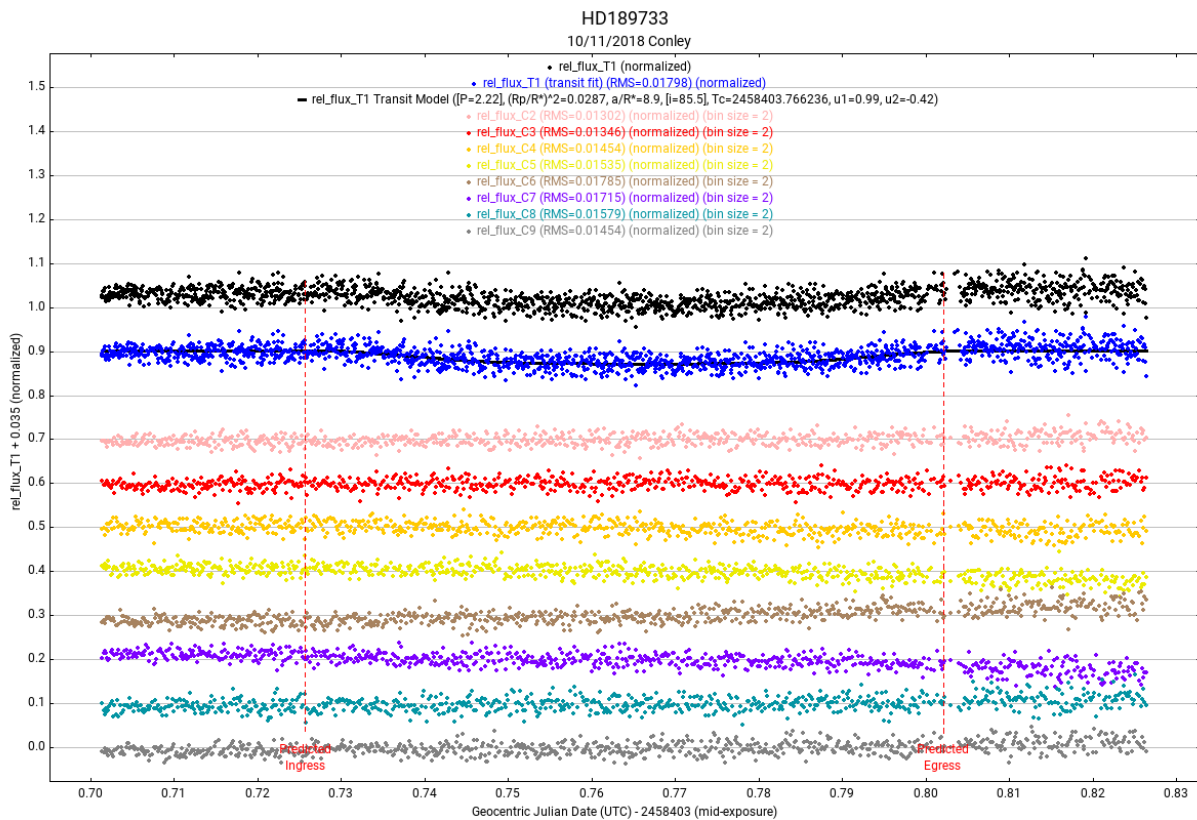


Figure 3.13. HD189733 light curve with 8 comparison stars, outliers removed. Black line represents transit fit. Red lines show the predicted start and end of the transit.

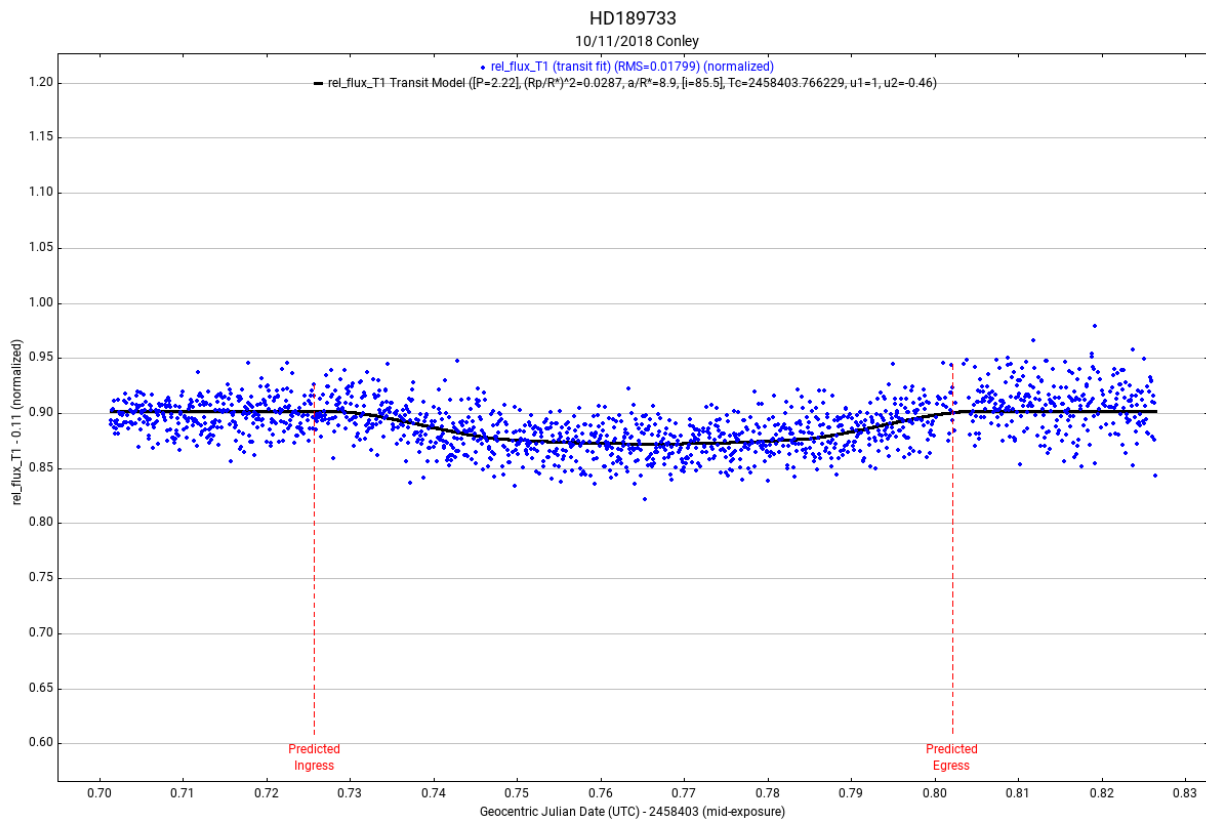


Figure 3.14. HD189733b light curve, outliers removed. Black line represents the transit fit. Red lines show the predicted start and end of the transit.

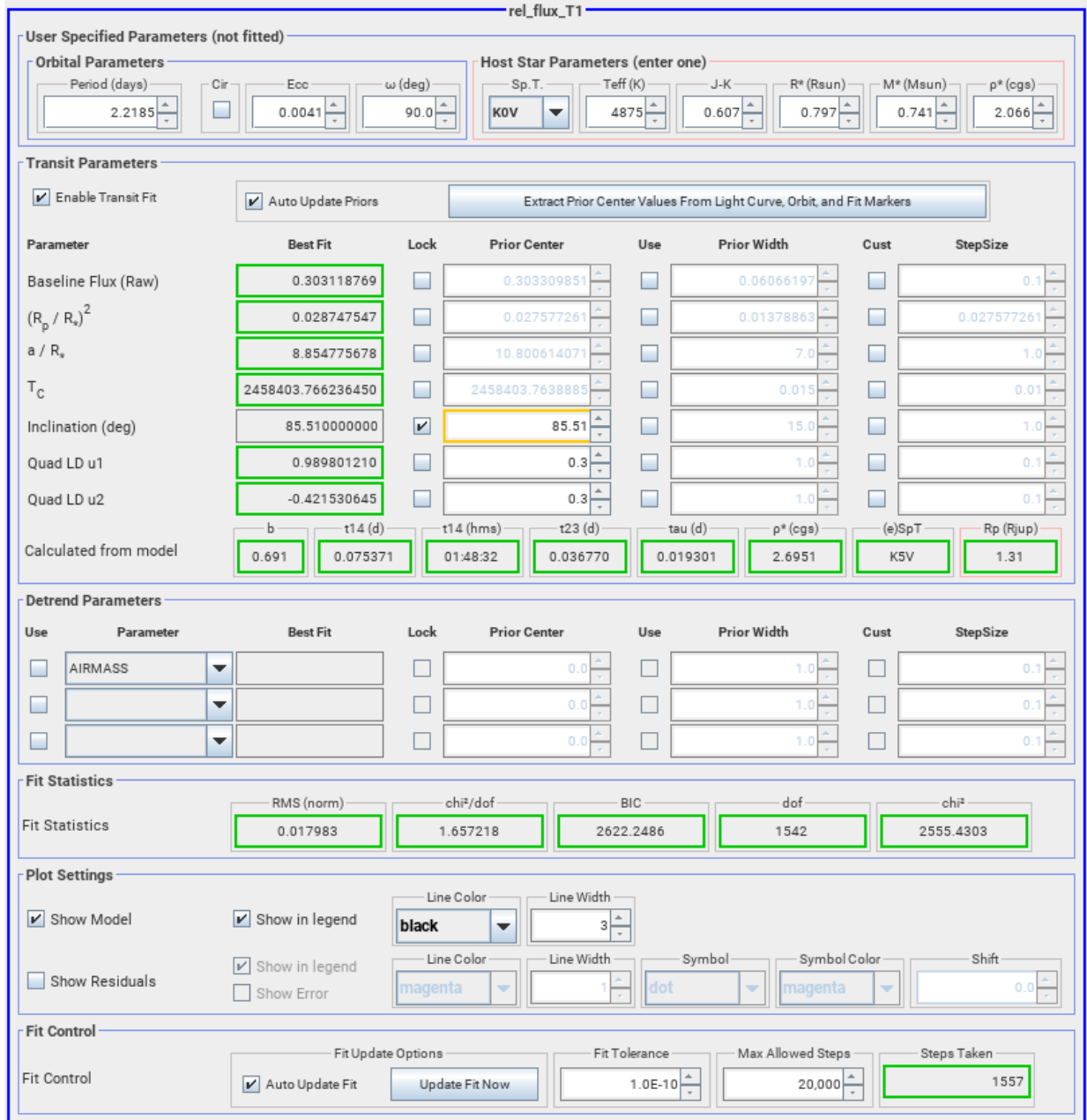


Figure 3.15. HD189733b model curve fit parameters. Data outliers removed.

Table 3.3.

HD189733b Measurements			
Value	Expected	Measured 10 Oct 2018	Measured 10 Oct 2018 (outliers removed)
Transit Depth (%)	$2.4 \pm .0058$ [32]	2.9	2.9
Transit Duration (min)	109.6 [30]	107.25	108.5
Transit Center (UT)	6:20 [30]	6:23:11	6:23:22
Planet Radius (R_{Jup})	$1.13 \pm .01$ [32]	1.32	1.31
R_p/R_*	$.116 \pm .01$ [32]	.17	.17

An observed transit depth of 2.9% was calculated on both data sets with and without outliers removed. This was close to the value of 2.4% observed by Stassun et al., 2017 [32]. The Transit durations of 107.25 min and 108.5min were calculated for data without and with outliers removed respectively. These were within 2 minutes of the ETD [30] published value for the transit duration. Observed transit center values were within 10 seconds of each other for the uncalibrated and outliers removed data, and within 3 minutes of the ETD [30] predicted time of 6:20 UT. The value of planetary radius was very close for both the uncalibrated and outliers removed data at $1.32 R_{Jup}$ and $1.31 R_{Jup}$ respectively. This was close to the published value of 1.13 by Stassun et al., 2017 [32]. Calculated values of R_p/R_* were identical for both sets of data (.17) and somewhat close to the published value of .116 [32]. Removing outliers from the HD189733b data set has resulted in the measurements for transit duration, transit center, and planetary radius moving closer to accepted values while other parameters were unchanged. It does appear to have improved the accuracy of this measurement in this single case.

CHAPTER 4

SUMMARY

Exoplanet observations of bright targets, $V \approx 7.6$ magnitude with transit depths of approximately 2% have been successfully demonstrated with the slightly modified CATE telescope systems for exoplanets HD209458b and HD189733b. Modifications to the scope system consist of adding an inexpensive guide scope, guide camera, and the addition of a micro controller system for pointing and guidance capability on the standard CG4 mount. In addition, the CATE observer needs to install the DEC motor to the CG4 mount that came with their original kit, and install and configure three free software packages; PHD2 [31] guiding software, AstroImageJ [9] or FITS Liberator [24] to view FITS files, and Astrometry.net [19] plate solving software. Observers utilize Fircapture image capture software already installed on their CATE laptop. Total cost for these modifications is \$600 as tested. It is also possible that volunteers who already own a computerized mount can install the CATE telescope on that mount for exoplanet observations.

Observations of HD189733b demonstrated much cleaner light curve plots than HD209458b, likely due to the amount of appropriate comparison stars in the FOV as well as the larger transit depth of 2.4% vs 1.5%. The CATE telescope FOV of 1 degree will limit the target stars CATE teams can look at due to the possible lack of appropriate comparison stars in the FOV. This is most evident in the observation of HD209458 where only one comparison star of similar magnitude is in the FOV. It is likely that we can successfully image transits at least down to magnitude 9 with similar transit depths of 1% or greater without image calibration. Observations of shallow transits of the TESS Earth and Super Earth candidates are likely not going to be possible for a single observer due to shallow transit depths on the order of .01%. By incorporating calibration images into the data collection and correcting for atmospheric attenuation over the course of the observation, it should be possible to achieve transit detection down to .1% [4] for a single telescope observation.

The strength in the Citizen CATE Experiment lies in the creation of the nationwide CATE telescope network operated by volunteers with identical equipment. While it has been shown that a single telescope can detect a transit of a relatively bright star, what remains to be demonstrated is the limit of the telescope network. Utilizing the full network to observe a single transit could result in a significant improvement over the sensitivity of a single scope. The network also has the possibility of lengthening the transit observation window. While a single scope could observe a transit for a maximum of 5-6 hours in duration [4], the CATE network stretching over 4 time zones can extend the transit observation window to 9-10 hours. The network would also offer significant redundancies in observations since local weather conditions would be minimized during a network wide observation. Follow up transit observations for the sake of keeping transit data fresh may be especially well suited for the CATE network due to their ability to conduct single observations of multiple bright targets in one night, or utilize the network to go after dimmer targets. The nature of the CATE volunteer network, made up mostly of educators and students, provides a unique opportunity to engage an evolving population of students in citizen science through exoplanet observations that have real scientific value.

REFERENCES

- [1] T. Boch and P. Fernique. Aladin Lite: Embed your Sky in the Browser. In N. Manset and P. Forshay, editors, *Astronomical Data Analysis Software and Systems XXIII*, volume 485 of *Astronomical Society of the Pacific Conference Series*, page 277, May 2014.
- [2] F. Bonnarel, P. Fernique, O. Bienaymé, D. Egret, F. Genova, M. Louys, F. Ochsenbein, M. Wenger, and J. G. Bartlett. The ALADIN interactive sky atlas. A reference tool for identification of astronomical sources. *Astronomy and Astrophysics*, 143:33–40, April 2000.
- [3] Francois Bouchy, Stephane Udry, Michel Mayor, Claire Moutou, Frederic Pont, Nicolas Iribarne, Ronaldo Da Silva, Sergio Ilovaisky, Didier Queloz, Nuno Santos, Damien Segransan, and Shay Zucker. ELODIE metallicity-biased search for transiting Hot Jupiters II. A very hot Jupiter transiting the bright K star HD189733. *Astronomy and Astrophysics*, 444, October 2005.
- [4] A. C. Cameron. *Extrasolar Planetary Transits*, volume 428 of *Astrophysics and Space Science Library*. Springer International Publishing Switzerland, 2016.
- [5] B. Campbell, G. A. H. Walker, and S. Yang. A Search for Substellar Companions to Solar-type Stars. *The Astrophysical Journal, Part 1*, 331:902, 1988.
- [6] D. Charbonneau, T. M. Brown, D. W. Latham, and M. Mayor. Detection of Planetary Transits Across a Sun-like Star. *The Astrophysical Journal*, 529:L45–L48, January 2000.
- [7] David Charbonneau, Timothy Brown, Adam Burrows, and Greg Laughlin. When Extrasolar Planets Transit Their Parent Stars. *Astrophysics*, March 2006.
- [8] A. Claret. A new non-linear limb-darkening law for LTE stellar atmosphere models. Calculations for $-5.0 \leq \log[M/H] \leq +1$, $2000 \text{ K} \leq T_{eff} \leq 50000 \text{ K}$ at several surface gravities. *Astronomy and Astrophysics*, 363:1081–1190, November 2000.
- [9] Karen A. Collins, John F. Kielkopf, Keivan G. Stassun, and Frederic V. Hessman.

ASTROIMAGEJ: IMAGE PROCESSING AND PHOTOMETRIC EXTRACTION FOR ULTRA-PRECISE ASTRONOMICAL LIGHT CURVES. *The Astronomical Journal*, 153(2):77, jan 2017.

- [10] Ian J. M. Crossfield, Heather Knutson, Jonathan Fortney, Adam P. Showman, Nicolas B. Cowan, and Drake Deming. Spitzer/MIPS 24 μ m OBSERVATIONS OF HD 209458b: THREE ECLIPSES, TWO AND a HALF TRANSITS, AND a PHASE CURVE CORRUPTED BY INSTRUMENTAL SENSITIVITY VARIATIONS. *The Astrophysical Journal*, 752(2):81, May 2012.
- [11] Jason Eastman, B. Scott Gaudi, and Eric Agol. EXOFAST: A Fast Exoplanetary Fitting Suite in IDL. *Publications of the Astronomical Society of the Pacific*, 125(923):83–112, January 2013.
- [12] Torsten Edelmann. FireCapture, version 2.6, 2018. URL = <http://www.firecapture.de>.
- [13] Eric B. Ford and Ji Wang. On the eccentricity distribution of short-period single-planet systems. *Monthly Notices of the Royal Astronomical Society*, 418(3):1822–1833, December 2011.
- [14] E. Han, S. X. Wang, J. T. Wright, Y. K. Feng, M. Zhao, O. Fakhouri, J. I. Brown, and C. Hancock. Exoplanet Orbit Database. II. Updates to Exoplanets.org. *Publications of the Astronomy Society of the Pacific*, 126:827, September 2014.
- [15] Artie P. Hatzes, William D. Cochran, Michael Endl, Barbara McArthur, Diane B. Paulson, Gordon A. H. Walker, Bruce Campbell, and Stephenson Yang. A Planetary Companion to Cephei A. *The Astrophysical Journal*, 599(2):1383–1394, dec 2003.
- [16] G. W. Henry, G. W. Marcy, R. P. Butler, and S. S. Vogt. A Transiting “51 Peg-like” Planet. *The Astrophysical Journal*, 529:L41–L44, January 2000.
- [17] Liam Dowling Jones, Lucas M. Marchioni, Scott G. Engle, Edward F. Guinan, and Joseph M. Michail. Evidence of a Decreasing Orbital Period for the Prototype Hot Jupiter System HD 189733: Implications for the Angular Momentum Evolution of Hot Jupiter Systems. *Research Notes of the AAS*, 2(1):36, March 2018.

- [18] C. Brooke Lamell, Debra A. Fischer, John Brewer, Pierre Demarque, Sarbani Basu, Tabettha Boyajian, Timothy R. White, Vicente Maestro, Federico Spada, Mercedes Lpez-Morales, Michael Ireland, Stephen R. Kane, Harold A. McAlister, Jeremy Jones, David R. Ciardi, Stephen Ridgway, Kaspar von Braun, Gerard T. van Belle, Gregory A. Feiden, Daniel Huber, Chris Farrington, Gail Schaefer, Laszlo Sturmann, Nils H. Turner, P. J. Goldfinger, Theo A. ten Brummelaar, and Andrew W. Mann. Stellar diameters and temperatures VI. High angular resolution measurements of the transiting exoplanet host stars HD 189733 and HD 209458 and implications for models of cool dwarfs. *Monthly Notices of the Royal Astronomical Society*, 447(1):846–857, December 2014.
- [19] Dustin Lang, David W. Hogg, Keir Mierle, Michael Blanton, and Sam Roweis. ASTROMETRY.NET: BLIND ASTROMETRIC CALIBRATION OF ARBITRARY ASTRONOMICAL IMAGES. *The Astronomical Journal*, 139(5):1782–1800, mar 2010.
- [20] Kaisey Mandel and Eric Agol. Analytic Light Curves for Planetary Transit Searches. *The Astrophysical Journal*, 580(2):L171–L175, dec 2002.
- [21] Timothy D. Morton, Stephen T. Bryson, Jeffrey L. Coughlin, Jason F. Rowe, Ganesh Ravichandran, Erik A. Petigura, Michael R. Haas, and Natalie M. Batalha. FALSE POSITIVE PROBABILITIES FOR ALLKEPLEROBJECTS OF INTEREST: 1284 NEWLY VALIDATED PLANETS AND 428 LIKELY FALSE POSITIVES. *The Astrophysical Journal*, 822(2):86, may 2016.
- [22] NASA. NASA Exoplanet Archive, 2018. URL = <https://exoplanetarchive.ipac.caltech.edu/index.html>.
- [23] NASA. TESS Science web page, 2019. URL = <https://heasarc.gsfc.nasa.gov/docs/tess/primary-science.html>.
- [24] Lars Holm Nielsen, Lars Lindberg Christensen, Robert Hurt, Kaspar K. Nielsen, and Teis Johansen. The ESA/ESP/NASA Photoshop FITS Liberator 3: Have your say on new features. In Lars Lindberg Christensen, Manolls Zoullas, and Ian Robson,

- editors, *Communicating Astronomy with the Public 2007*, pages 486–488, Athens Greece, October 2007. Communicating Astronomy with the Public.
- [25] M. Penn, B. Baer, and F. Isberner. Citizen CATE Experiment: Prototype Testing and Plans. *Society for Astronomical Sciences Annual Symposium*, 34:63–68, May 2015.
- [26] M J Penn, R Baer, R Bosh, D Garrison, R Gelderman, H Hare, F Isberner, L Jensen, S Kovac, M McKay, A Mitchell, M Pierce, P Thompson, A Ursache, J Varsik, D Walter, Z Watson, and D Young and. Instrumentation for the Citizen CATE Experiment: Faroe Islands and Indonesia. *Publications of the Astronomical Society of the Pacific*, 129(971):015005, dec 2016.
- [27] Simon C. Schuler, Davin Flateau, Katia Cunha, Jeremy R. King, Luan Ghezzi, and Verne V. Smith. ABUNDANCES OF STARS WITH PLANETS: TRENDS WITH CONDENSATION TEMPERATURE,. *The Astrophysical Journal*, 732(1):55, April 2011.
- [28] S. Seager and G. Mallen-Ornelas. A Unique Solution of Planet and Star Parameters from an Extrasolar Planet Transit Light Curve. *The Astrophysical Journal*, 585(2):1038–1055, March 2003.
- [29] John Southworth. Homogeneous studies of transiting extrasolar planets III. Additional planets and stellar models. *Monthly Notices of the Royal Astronomical Society*, 408(3):1689–1713, October 2010.
- [30] Variable Star and Exoplanet Section of the Czech Astronomical Society. Exoplanet Transit Database, 2018. URL = <http://var2.astro.cz/ETD/>.
- [31] Craig Stark. Autoguiding: As Simple as, "Push Here Dummy"? *Astronomy Technology Today*, pages 47–56, October 2007.
- [32] Keivan G. Stassun, Karen A. Collins, and B. Scott Gaudi. Accurate Empirical Radii and Masses of Planets and Their Host Stars with Gaia Parallaxes. *The Astronomical Journal*, 153(3):136, mar 2017.
- [33] Triaud, A. H. M. J., Collier Cameron, A., Queloz, D., Anderson, D. R., Gillon, M.,

Hebb, L., Hellier, C., Loeillet, B., Maxted, P. F. L., Mayor, M., Pepe, F., Pollacco, D., Ségransan, D., Smalley, B., Udry, S., West, R. G., and Wheatley, P. J. Spin-orbit angle measurements for six southern transiting planets - New insights into the dynamical origins of hot Jupiters. *A&A*, 524:A25, 2010.

[34] Jason Wei. A Survey of Exoplanetary Detection Techniques. *Astrophysics Earth and Planetary*, May 2018. URL = <https://arxiv.org/abs/1805.02771>.

[35] M. Wenger, F. Ochsenbein, D. Egret, P. Dubois, F. Bonnarel, S. Borde, F. Genova, G. Jasniewicz, S. Laloë, S. Lesteven, and R. Monier. The SIMBAD astronomical database. The CDS reference database for astronomical objects. *Astronomy and Astrophysics*, 143:9–22, April 2000.

VITA

Graduate School
Southern Illinois University

Robert Baer

rbaer@siu.edu

Illinois State University
Bachelor of Science, Physics, May 1995

Special Honors and Awards: SIUC Staff Excellence Award, 2017

Thesis Paper Title:

OBSERVING EXOPLANET TRANSITS WITH THE CITIZEN
CONTINENTAL-AMERICA TELESCOPIC ECLIPSE (CATE) EXPERIMENT
TELESCOPE NETWORK

Major Professor: Dr. M. Byrd

Publications:

Robert T. Zellem, Anya Biferno, David R. Ciardi, Mary Dussault, Laura Peticolas, Martin Fowler, Kyle A. Pearson, Wilfred Gee, Rachel Zimmerman-Brachman, Denise Smith, Lynn Cominsky, Gael M. Roudier, Brandon Lawton, Robert Baer, Diana Dragomir, Nemanja Jovanovic, Marc Kuchner, Frank Sienkiewicz, Josh Walawender, Engaging Citizen Scientists to Keep Transit Times Fresh and Ensure the Efficient Use of Transiting Exoplanet Characterization Missions, *White Paper submitted to Astro2020 Science Call*, URL: <https://arxiv.org/abs/1903.07716>, 2019

Bosh, Robert; Penn, Matthew J.; McKay, Myles; Baer, Robert; Garrison, David; Gelderman, Richard; Hare, Honor; Isberner, Fred; Jensen, Logan; Kovac, Sarah; Mitchell, Adriana; Pierce, Michael; Thompson, Patricia; Ursache, Andrei; Varsik, John R.; Walter, Donald K.; Watson, Zachary; Young, David; Citizen Cate Team, Multi-site Observations of the March 2016 Total Solar Eclipse: Calibration of Images to Simulate Continuous Monitoring, *American Astronomical Society, AAS Meeting #229*, URL: <http://adsabs.harvard.edu/abs/2017AAS...22942401B>, 2017

Mitchell, Adriana; Penn, Matt; Baer, Robert; Bosh, Robert; Garrison, David; Gelderman, Richard; Hare, Honor; Isberner, Fred; Jensen, Logan; Kovac, Sarah; McKay, Myles; Pierce, Michael; Thompson, Patricia; Ursache, Andrei; Varsik, John R.; Walter, Donald; Watson, Zachary; Young, David; Citizen CATE Team, Citizen CATE Experiment and Polar Plume Dynamics, *American Astronomical Society Meeting Abstracts #229*, URL:

<http://adsabs.harvard.edu/abs/2017AAS...22933907M>. 2017

McKay, Myles; Penn, Matt; Baer, Robert; Bosh, Robert; Garrison, David; Gelderman, Richard; Hare, Honor; Isberner, Fred; Jensen, Logan; Kovac, Sarah; Mitchell, Adriana; Pierce, Michael; Thompson, Patricia; Ursache, Andrei; Varsik, John R.; Walter, Donald K.; Watson, Zachary; Young, David T.; Citizen CATE Team, Update on the Citizen CATE Experiment: Indonesia to 2017, *American Astronomical Society Meeting Abstracts*, <https://ui.adsabs.harvard.edu/#abs/2017AAS...22914002M>, 2017

Penn, M., Baer, R., Bosh, R., Garrison, D., Gelderman, R., Hare, H., Isberner, F., Jensen, L., Kovac, S., McKay, M., Mitchell, A., Pierce, M., Ursache, A., Varsik, J., Walter, D., Watson, Z., Young, D., Instrumentation for the Citizen CATE Experiment: Faroe Islands and Indonesia, *Publications of the Astronomical Society of the Pacific*, <https://arxiv.org/abs/1609.00035>, 2016

Penn, M. J.; McKay, M. A.; Kovac, S. A.; Jensen, L.; Hare, H. S.; Mitchell, A. M.; Bosh, R.; Watson, Z.; Baer, R.; Pierce, M.; Gelderman, R.; Walter, D. K., CATE 2016 Indonesia: Science goals and student training for 2017, *AGU Fall Meeting Abstracts*, <https://ui.adsabs.harvard.edu/#abs/2016AGUFMED42A..03P>, 2016

Penn, M. and Baer, B. and Isberner, F., Citizen CATE Experiment: Prototype Testing and Plans, *Society for Astronomical Sciences Annual Symposium*, 2015, 34, 63-68, <http://adsabs.harvard.edu/abs/2015SASS...34...63P>

Determination of Magnetic Phase Transitions in Holmium Using Magnetoresistance Measurements. J. R. Gebhardt, R. A. Baer, and Naushad Ali. Department of Physics, Southern Illinois University at Carbondale. *Journal of Alloys and Compounds*, 250 (1997) 655-658.

Affiliations:

Staff member, Physics Department, SIU Carbondale.

NASA Science Mission Directorate (SMD) Member. URL: <https://smdepo.org/user/1023>

Grants:

National Aeronautics and Space Administration, SMD NNX16AB92A, "Geographically distributed citizen scientist training for the 2017 Citizen CATE Experiment," 2015.

National Science Foundation, 1732227, "The Citizen CATE (Continental-America Telescope Eclipse) Experiment to Observe the 2017 Great American Eclipse," 2017.